5880 J. Med. Chem. 2009, 52, 5880–5895
DOI: 10.1021/jm9005302

Journal of Medicinal Chemistry Article

Structure-Based Optimization of Arylamides as Inhibitors of Soluble Epoxide Hydrolase†

Anne B. Eldrup,*,‡ Fariba Soleymanzadeh,‡ Steven J. Taylor,‡ Ingo Muegge,‡ Neil A. Farrow,‡ David Joseph,§ Keith McKellop,∥ Chuk C. Man,‡ Alison Kukulka,‡ and Stéphane De Lombaert‡

‡Department of Medicinal Chemistry, Boehringer Ingelheim Pharmaceuticals, Ridgefield, Connecticut 06877, §Department of Drug Discovery Support, Boehringer Ingelheim Pharmaceuticals, Ridgefield, Connecticut 06877, and ∥Department of Analytical Sciences, Boehringer Ingelheim Pharmaceuticals, Ridgefield, Connecticut 06877

Received April 24, 2009

Inhibition of soluble epoxide hydrolase (sEH) is hypothesized to lead to an increase in circulating levels of epoxyeicosatrienoic acids, resulting in the potentiation of their in vivo pharmacological properties. As part of an effort to identify inhibitors of sEH with high and sustained plasma exposure, we recently performed a high throughput screen of our compound collection. The screen identified *N*-(3,3-diphenyl-propyl)-nicotinamide as a potent inhibitor of sEH. Further profiling of this lead revealed short metabolic half-lives in microsomes and rapid clearance in the rat. Consistent with these observations, the determination of the in vitro metabolic profile of *N*-(3,3-diphenyl-propyl)-nicotinamide in rat liver microsomes revealed extensive oxidative metabolism and a propensity for metabolite switching. Lead optimization, guided by the analysis of the solid-state costructure of *N*-(3,3-diphenyl-propyl)-nicotinamide bound to human sEH, led to the identification of a class of potent and selective inhibitors. An inhibitor from this class displayed an attractive in vitro metabolic profile and high and sustained plasma exposure in the rat after oral administration.

Introduction

Cytochrome P450-mediated epoxidation of arachidonic acid yields four regioisomeric epoxyeicosatrienoic acids (EETs[a]) that display vasodilatory, antiinflammatory, and analgesic, as well as migratory and proliferative properties.[1−3] The intriguing biological properties and complex biology of EETs have drawn attention to the role of soluble epoxide hydrolase (sEH) as the enzyme primarily responsible for the further metabolic conversion of these regioisomeric epoxides (Figure 1).[4,5]

Soluble epoxide hydrolase (sEH) promotes the hydrolysis of EETs to their pharmacologically less active and more rapidly cleared dihydroxy epoxyeicosatrienoic acids (DHETs).[6] Researchers have hypothesized that the selective inhibition of sEH will lead to an increase in circulating levels of EETs, resulting in the potentiation of their in vivo pharmacological properties.[1,2] In accordance with this hypothesis, several reports have been published that demonstrate efficacy of small molecule inhibitors of sEH in cardiovascular animal models and in models of inflammation.[7−9]

We recently decided to determine the potential of sEH inhibitors as vasodilators and as cardio- or renal-protective agents. At the onset of our studies, two potent sEH inhibitors, 1-cyclohexyl-3-dodecylurea (CDU) and 12-(3-adamantan-1-yl-ureido)dodecanoic acid (AUDA), had been extensively utilized as tool compounds (Figure 2). Common structural features of these inhibitors are the large hydrophobic domains flanking their central urea pharmacophore.[10−14] Reasoning that these large hydrophobic domains may limit the "drug-like" characteristics and pharmacokinetic properties of these compounds, we elected to perform a high-throughput screen of our in-house compound collection in order to identify a structurally different starting point for an optimization process. *N*-(3,3-Diphenyl-propyl)-nicotinamide (Figure 3, **1**) was identified as a potent inhibitor of sEH and selected as the starting point for lead optimization. Optimization of **1** was guided by the analysis of its in vitro metabolic profile and by the close examination of its solid-state structure when bound to human sEH. Our analysis led to the identification of a new class of functionalized 3,3-diphenylpropylamine arylamides that are potent inhibitiors of sEH activity in both molecular and cell-based assays. A compound from this class, 4-cyano-*N*-[3-(4-fluorophenyl)-3-(4-methanesulfonyl-phenyl)-propyl]-benzamide (**24**), was found to display attractive stability profiles in rat and human liver microsomes and high and sustained plasma exposure in the rat after oral administration.

Chemistry

The identified lead *N*-(3,3-diphenyl-propyl)-nicotinamide (**1**) was resynthesized from nicotinic acid and (3,3-diphenyl-propyl)-amine using hydroxybenzotriazole, 1-[3-(dimethyl-amino)propyl]-3-ethylcarbodiimide, and Hunig's base in dimethylformamide, as described in the general procedure for amide coupling. Our initial SAR focused on structural modifications to define an optimized scaffold for sEH inhibition (Tables 1−3). Subsequent chemical functionalizations were

†PDB files for the complexes soluble epoxide hydrolase and inhibitors **1** and **24** (PDB identifiers 3I1Y and 3I28, respectively) have been deposited with the Protein Data Bank.

*To whom correspondence should be addressed. Phone: 203 798 5658. Fax: 203 791 6072. E-mail: anne.eldrup@boehringer-ingelheim.com.

[a] Abbreviations: sEH, soluble epoxide hydrolase; EETs, epoxyeicosatrienoic acids; DHETs, dihydroxy epoxyeicosatrienoic acids; CDU, 1-cyclohexyl-3-dodecylurea; AUDA, 12-(3-adamantan-1-yl-ureido)dodecanoic acid; CIU, *N*-cyclohexyl-*N*′-(4-iodophenyl) urea.

 Published on Web 09/11/2009

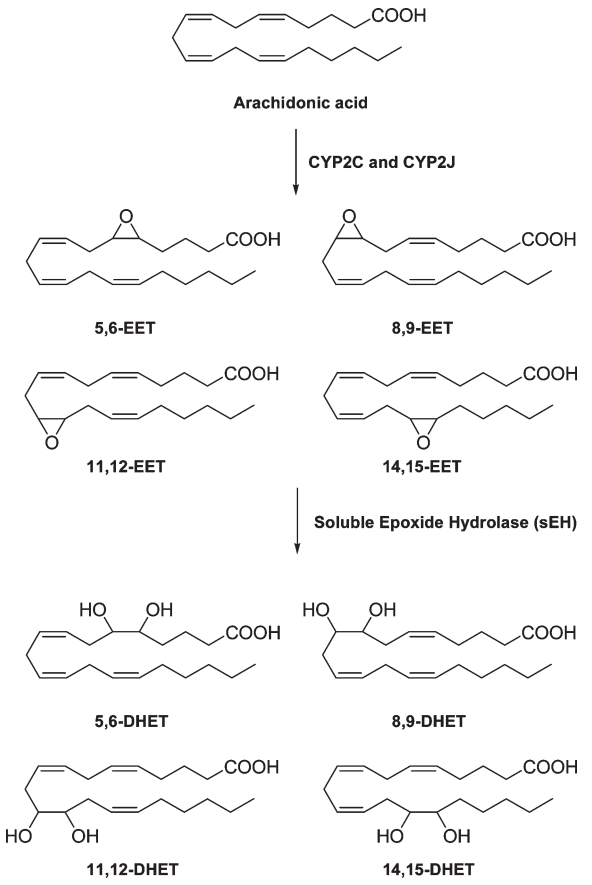

Figure 1. Cytochrome P450-mediated epoxidation of arachidonic acid yields four regioisomeric epoxyeicosatrienoic acids (EETs). EETs are further metabolized by soluble epoxide hydrolase (sEH) to yield their corresponding and generally less active vicinal dihydroxy epoxyeicosatrienoic acids (DHETs). Inhibition of sEH selectively over the CYP 450 expoxygenases has been hypothesized to lead to an increase in circulating EETs levels, resulting in the potentiation of their in vivo beneficial pharmacological effects.

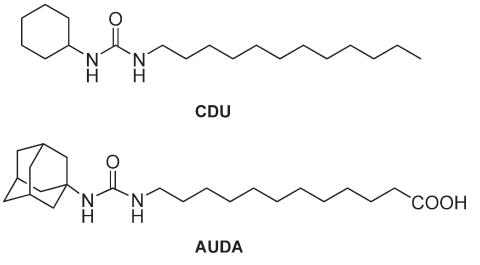

Figure 2. Recent studies of structurally simple inhibitors of soluble epoxide hydrolase, such as 1-cyclohexyl-3-dodecylurea (CDU) and 12-(3-adamantan-1-yl-ureido)dodecanoic acid (AUDA) (Figure 2), has confirmed a role for the inhibition of sEH in both cardiovascular and inflammatory diseases. Common structural features of these inhibitors are the large hydrophobic domains flanking the central urea pharmacophore, which may limit the "drug-like" characteristics of these compounds.

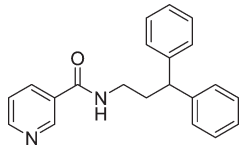

Figure 3. Chemical structure of the sEH inhibitor, *N*-(4,4-diphenylpropyl)-nicotinamide (**1**), identified through high throughput screening.

Table 1. Inhibitory Potency (IC_{50}) against sEH and Stability in Microsomes ($t_{1/2}$) for Compounds **2**−**5** Compared to Compound **1**[a]

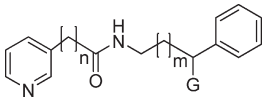

	G	n	m	human sEH IC_{50} [nM]	rat sEH IC_{50} [nM]	hLM $t_{1/2}$ [min]	rLM $t_{1/2}$ [min]
1	Ph	0	1	7.0	4.8	13	3
2	Ph	0	0	> 3000	> 3000	4	4
3	Ph	0	2	120	26	6	3
4	H	0	1	700	70	105	76
5	Ph	1	1	31.0	150	4	4

[a] Compounds were designed to examine the effect a change in the length of the linker to right-hand side benzhydryl pharmacophore, the importance of the benzhydryl motif, and effect of a transposition of the left-hand side 3-pyridiyl motif.

Table 2. Inhibitory Potency (IC_{50}) against sEH for Compounds **6** and **7** Compared to Compound **1**[a]

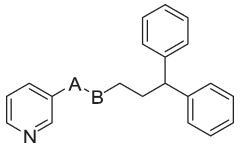

	A	B	human sEH IC_{50} [nM]	rat sEH IC_{50} [nM]
1	C(O)	NH	7.0	4.8
6	NH	C(O)	45	18
7	$S(O)_2$	NH	> 3000	> 3000

[a] Compounds were designed to examine the effect reversing the central amide pharmacophore or replacing it with a sulfonamide moiety.

designed to improve metabolic stability. Standard methods for chemical synthesis and commercial starting materials were used unless otherwise described (see below and Experimental Section).

The effect of a change in the tether length between the amide pharmacophore and the benzhydryl motif of *N*-(3,3-diphenylpropyl)-nicotinamide **1** was investigated by the synthesis of the 2,2-diphenylethyl and 4,4-diphenylbutyl derivatives (Table 1, entries **2** and **3**). 4,4-Diphenylbutylamine, required for the synthesis of compound **3**, was available according to literature procedures.[15] The importance of the right-hand side benzhydryl motif was investigated by the synthesis of its 3-phenylpropyl analogue in which one phenyl is omitted (Table 1, entry **4**). In addition, the effect of a transposition of the left-hand side 3-pyridiyl pharmacophore by insertion of a methylene spacer was investigated by the synthesis of the 3-pyridylacetamide analogue of **1** (Table 1, entry **5**).

To define the importance of the central amide pharmacophore, compounds were synthesized in which the amide configuration was either reversed (Table 2, entry **6**) or replaced by a sulfonamide (Table 2, entry **7**). The prerequisite 4,4-diphenyl-butyric acid for the synthesis of compound **6** was prepared from 4-phenyl-butyrolactone, benzene, and aluminum chloride according to the described literature procedure.[16]

The effect of transposition or omission of the left-hand side pyridyl heteroatom of **1** was examined by preparing its regioisomeric 2-pyridyl and 4-pyridyl analogues (Table 3,

Table 3. Inhibitory Potency (IC_{50}) against sEH and Stability in Microsomes ($t_{1/2}$) for Compounds **8**−**10** Compared to Compound **1**[a]

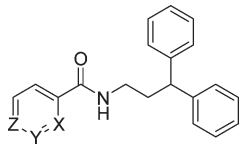

	X	Y	Z	human sEH IC_{50} [nM]	rat sEH IC_{50} [nM]	hLM $t_{1/2}$ [min]	rLM $t_{1/2}$ [min]
8	N	CH	CH	100	43	8	4
1	CH	N	CH	7.0	4.8	13	3
9	CH	CH	N	7.9	7.6	3	5
10	CH	CH	CH	5.1	7.2	5	3

[a] Compounds were designed to examine the effect of either a transposition or an omission of the left-hand side pyridyl heteroatom.

entries **8** and **9**) and by synthesizing the corresponding benzamide analogue in which the heteroatom is omitted (Table 3, entry **10**).

Our profiling of compounds **1**−**10** defined *N*-(3,3-diphenylpropyl)-arylamide as a preferred scaffold for sEH inhibition (Tables 1−3), and subsequent chemical functionalizations were carried out to improve the poor in vitro metabolic stability of this compound class (see Results and Discussion Section). The effect of polar substituents on the left-hand side aromatic ring system was examined through the synthesis of the nicotinamide (**11**), 6-hydroxy-nicotinamide (**12**), 6-(2,2,2-trifluoro-ethoxy)-nicotinamide (**13**), 2-(2,2,2-trifluoro-ethoxy)-isonicotinamide (**14**), 4-cyano-benzamide (**15**), and 4-methanesulfonyl-benzamide (**16**) derivatives in the context of a bis-(4-fluorophenyl)-modified benzhydryl right-hand side motif (Table 4, entries **11**−**16**). The prerequisite 3,3-bis-(4-fluorophenyl)-propylamine for these transformations was prepared similarly to published methods.[17] Briefly, 4,4′-difluorobenzophenone was reacted with the anion of acetonitrile to give 3,3-bis-(4-fluorophenyl)-3-hydroxypropionitrile, which upon reduction with lithium aluminum hydride and aluminum trichloride gave the desired 3,3-bis-(4-fluorophenyl)-propylamine.

On the basis of our analysis of the solid-state structure of **1** bound to human sEH, and in a further effort to improve metabolic stability profiles for this compound class, the synthesis of inhibitors with unsymmetrically substituted benzhydryl right-hand sides was undertaken (Table 5, entries **21**−**25**). Access to the desired 3-(4-fluorophenyl)-3-(4-methanesulfonyl-phenyl)-propylamine intermediate (**20**) proceeded via a $Pd_2(dba)_3$ mediated Suzuki−Miyaura cross-coupling reaction between 4-(methanesufonyl)benzeneboronic acid and 3-chloro-3-(4-fluorophenyl)-acrylonitrile (Scheme 1, **17**) as we have previously reported.[18] The resulting unsymmetrically substituted acrylonitrile (**18**) was subjected to catalytic hydrogenation in the presence of di-*tert*-butyl dicarbonate to give the *t*-Boc-protected propylamino derivative (**19**). Removal of the *t*-Boc group gave the desired propylamino intermediate, **20**, after treatment with aqueous hydrochloric acid in methanol. The effect of this unsymmetrical functionalization of the benzhydryl motif was assessed by the synthesis of a similar set of substituted nicotinic and benzoic acids as examined for the bis-(4-fluorophenyl) modified benzhydryl motif (Table 5, entries **21**−**25**).

To fully exploit the fact that the aromatic rings of the benzhydryl motif experience different electronic environments within the protein (see Results and Discussion Section), the

Table 4. Inhibitory Potency (IC_{50}) against sEH and Stability in Microsomes ($t_{1/2}$) for Compounds **11**−**16**[a]

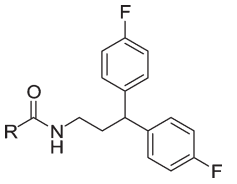

	R	human sEH IC_{50} [nM]	rat sEH IC_{50} [nM]	hLM / rLM $t_{1/2}$ [min]
11		8	7	12/12
12		5	9	110/22
13	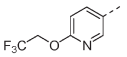	5	6	>300/>300
14	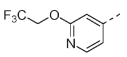	5	7	139/5
15		5	7	33/5
16		5	7	47/5

[a] Compounds were designed to examine the effect of polar substituents on the left-hand side aromatic ring system in the context of a bis-(4-fluorophenyl)-modified benzhydryl right-hand side motif.

synthesis of optically pure analogues was undertaken (Scheme 2 and Table 5, entries **S-24**, **R-24**, **S-22**, and **R-22**). The prerequisite (*S*)- and (*R*)-3-(4-fluorophenyl)-3-(4-methanesulfonyl-phenyl)-propylamines **34a** and **34b** were accessed from 4-fluorocinnamic acid (**26**) by coupling to the appropriate chiral auxiliary, (*R*)-(−)-4-phenyl-2-oxazolidinone or (*S*)-(+)-4-phenyl-2-oxazolidinone (Scheme 2). Couplings proceeded via the in situ formation of the mixed anhydrides, using pivaloyl chloride and triethylamine in tetrahydrofuran, to give the desired 3-[3-(4-fluorophenyl)-acryloyl]-(*R*)-4-phenyl-oxazolidin-2-one (**27a**) and 3-[3-(4-fluorophenyl)-acryloyl]-(*R*)-4-phenyl-oxazolidin-2-one (**27b**). Chiral functionalization to give the (*R*,*R*)- and (*S*,*S*)-diastereoisomeric 4-methanesulfanylphenyl oxazolidinone intermediates **28a** and **28b** proceeded from **27a** and **27b** via an asymmetric conjugate addition using the in situ generated organocopper reagent available by reaction of thioanisole magnesium bromide with copper(I)bromide−methylsulfide complex in tetrahydrofuran. The removal of the chiral auxiliary was performed under standard conditions, with sodium borohydride in a mixture of tetrahydrofuran and water, to give the optically pure alcohols **29a** and **29b**. Further chemical transformation of these alcohols to their corresponding azides **30a** and **30b** was accomplished by reaction with toluenesulfonyl chloride in the presence of triethylamine in dichloromethane, followed by the replacement of the tosylate using sodium azide in

Table 5. Inhibitory Potency (IC_{50}) against sEH, Cell-Based Potency (EC_{50}), and Stability in Microsomes ($t_{1/2}$) for Compounds **21**−**25**[a]

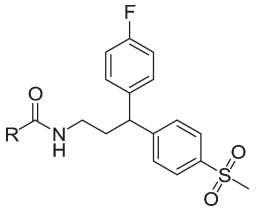

	R	human sEH IC_{50} [nM]	rat sEH IC_{50} [nM]	Hep G2 EC_{50} [nM]	hLM / rLM $t_{1/2}$ [min]
21		8	14	0.6	6/12
22		16	29	2.1	157/>300
23	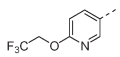	4	6	0.3	> 300/150
24		6	9	0.3	> 300/150
25		7	8	0.4	> 300/161

[a] Compounds were designed to examine the effect of polar substituents on the left-hand side aromatic ring system in the context of an unsymmetrically methanesulfonyl substituted benzhydryl right-hand side.

N,*N*′-dimethylformamide. The resulting azide intermediates 30a and **30b** were treated with a mixture of aqueous hydrogen peroxide and glacial acetic acid to give **31a** and **31b**, respectively. Subsequent catalytic reduction in methanol gave the methanesulfoxide-functionalized *t*-Boc-protected propylamino derivatives **32a** and **32b** after treatment with di-*tert*-butyl dicarbonate. Oxidation of the methanesulfoxides **32a** and **32b** was accomplished by the treatment with oxone in the presence of aluminum oxide to afford the methanesulfoxide derivatives **33a** and **33b**, which were subjected to treatment with trifluoroacetic acid to afford the desired *R*- and *S*-enantiomers of 3-(4-fluorophenyl)-3-(4-methanesulfonyl-phenyl)-propylamine, **34a** and **34b**, respectively.

Results and Discussion

N-(3,3-Diphenyl-propyl)-nicotinamide (Figure 3, **1**) was identified as a potent inhibitor of sEH through high throughput screening. Further profiling of this lead compound revealed short half-lives in both human and rat liver microsomes and rapid clearance in the rat (data not shown). A lead optimization process was undertaken with the goal to improve in vitro metabolic stability as an avenue to identify compounds with high and sustained plasma exposure in the rat. Compounds were evaluated in binding assays for their ability to displace a rhodamine-labeled probe from either human or rat sEH using a fluorescence polarization readout (see Experimental Section for methods). Selected compounds were assessed for their ability to inhibit the sEH-mediated conversion of 14,15-epoxyeicosatienoic acid to 14,15-dihydroxyeicosatrienoic acid in human Hep G2 cells using an ELISA readout. Metabolic stability was an important driver of the SAR for this compound class, and for selected compounds, half-lives in human and rat liver microsomes were determined as a measure of first-pass metabolism (see Experimental Section for methods). Compound exposure in rat was assessed after oral administration at 1, 2, 4, and 6 h post dosing (see Experimental Section for methods).

Scheme 1. Synthetic Route to 3-(4-Fluorophenyl)-3-(4-methanesulfonyl-phenyl)-propyl Amine (**20**)[a]

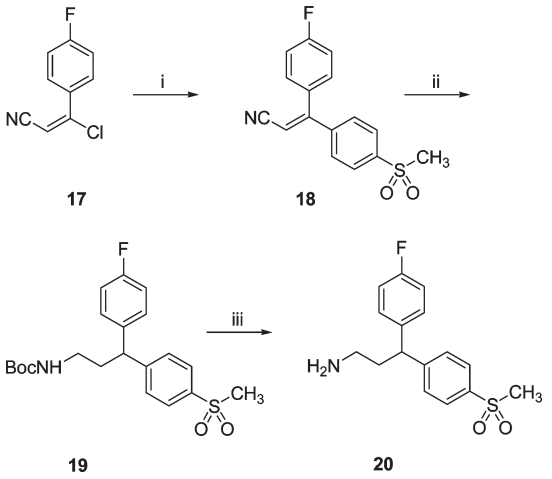

[a] Reagents and conditions: (i) (4-methanesulfonyl)benzeneboronic acid, $[(t\text{-Bu})_3PH]BF_3$, $Pd_2(dba)_3$, and KF in tetrahydrofuran overnight at 45°C; (ii) di-*tert*-butyl dicarbonate and Pd/C in methanol shaken under hydrogen at 50 psi for 24 h at room temperature; (iii) HCl in methanol, then *p*-toluenesulfonic acid 1 h at room temperature.

In an initial set of compounds, the length of the linker between the central amide pharmacophore and the right-hand side benzhydryl motif was varied from ethyl through propyl to butyl, leading to the finding that the propyl linker is optimal for inhibitory potency (Table 1, entries **1**−**3**). Truncation to the ethyl-linked derivative resulted in complete loss of activity (IC_{50} > 3000 nM for both human and rat sEH), whereas the extension of the propyl linker by one methylene unit resulted in a 17-fold decline in potency against human sEH (IC_{50} 120 nM) and a 4-fold decline in potency against the rat sEH isoform (IC_{50} 26 nM). The importance of the benzhydryl pharmacophore for potent sEH inhibition was demonstrated by the omission of a phenyl ring from this motif to give the 3-phenyl propylamide analogue (Table 1, entry **4**). This compound displayed large declines in inhibitory potency for both sEH isoforms (IC_{50} 700 and 70 nM for the human and rat isoforms, respectively). The transposition of the left-hand side pyridyl moiety by one methylene unit was examined by the evaluation of the 3-pyridylacetamide compound, **5**, which displayed a moderate inhibitory effect on sEH activity (IC_{50} 31 and 150 nM for the human and rat isoforms, respectively). In another set of compounds, the amide pharmacophore of **1** was either reversed or replaced with a sulfonamide (Table 2, entries **6** and **7**). The potency of the compound in which the amide was reversed was moderately reduced compared to **1** (IC_{50} 45 and 18 nM, for the human and rat isoforms, respectively). The compound in which the amide pharmacophore was replaced with sulfonamide completely lost its ability to inhibit sEH activity (see below for an analysis of this finding). Taken together, these findings (Tables 1 and 2) suggest that the benzhydryl motif is an important pharmacophore

Scheme 2. Synthetic Route to (*S*)-3-(4-Fluorophenyl)-3-(4-methanesulfonyl-phenyl)-propyl Amine (**S-20**) from 4-Fluorocinnamic Acid Using the Chiral Auxiliary (*R*)-(−)-4-Phenyl-2-oxazolidinone[a]

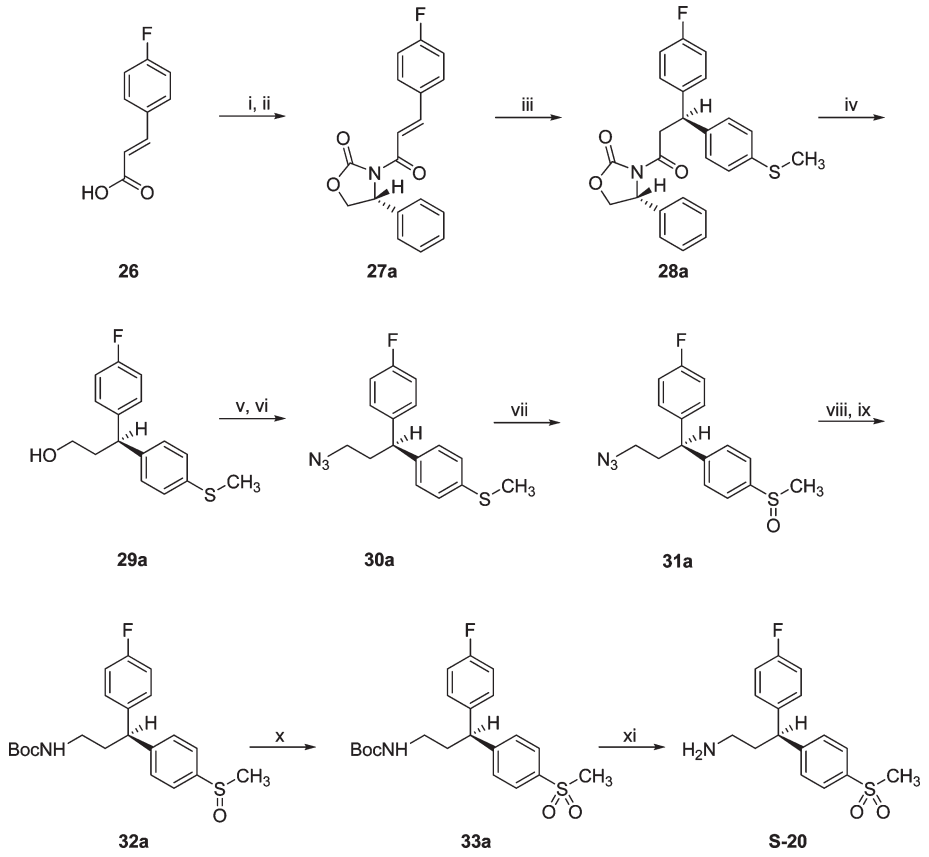

[a] (*R*)-3-(4-Fluorophenyl)-3-(4-methanesulfonyl-phenyl)-propyl amine (**R-20**) was prepared similarly starting from the enantiomeric (*S*)-(+)-4-phenyl-2-oxazolidinone. Reagents and conditions: (i) pivaloyl chloride and triethylamine in tetrahydrofuran at 0°C; (ii) pre-formed anion of (*R*)-(−)-4-phenyloxazolidinone (formed with lithium diisopropylamide (2M in tetrahydrofuran at −78°C) at −20°C to room temperature for 1 h; (iii) CuBr−methylsulfide complex, dimethylsulfide, and thioanisole methylmagnesium bromide in tetrahydrofuran at −40°C to room temperature overnight; (iv) sodium borohydride in water/tetrahydrofuran for 22 h at room temperature; (v) tosyl chloride and triethylamine in dichloromethane at −10°C to room temperature overnight; (vi) sodium azide in *N*,*N*′-dimethylformamide overnight at room temperature; (vii) aq hydrogen peroxide (30%) and glacial acetic acid at room temperature for 24 h; (viii) Pd/C in methanol, stirred under hydrogen for 4 h; (ix) Boc-anhydride, triethyl amine, 4 h at rt; (x) Al_2O_3, oxone, 24 h at reflux; (xi) HCl, then *p*-toluenesulfonic acid.

for sEH and that both its phenyl ring systems contribute to the molecular recognition of the enzyme. Moreover, the data indicates that the exact position of the central amide pharmacophore relative to the benzhydryl motif is crucial for inhibition of sEH activity by this class of compounds, probably reflecting a relatively tight fit of the benzhydryl moiety with the enzyme.

To better understand the molecular basis for the observed inactivity of the sulfonamide analogue (**7**), this compound was docked into the structure of human sEH obtained in-house with compound **1** cocrystallized (vide supra and Figure 5a,b for solid-state structure and Figure 4a,b for docking studies). Compound **7** was docked into the catalytic site using the program Glide assuming the same binding mode and exhibiting the same hydrogen bonding interaction pattern with the enzyme as observed for the benzamide **1** (Figure 4). Among a variety of docking conformations that differed slightly in how the sulfonamide atoms interacted with Asp 335, Tyr 383, and Tyr 466, a high energy *trans* (Figure 4a) and low energy *cis* (Figure 4b) sulfonamide conformation generated the highest docking scores.[19] The high energy *trans* sulfonamide displayed hydrogen bonding interaction patterns between the sulfonamide moiety and sEH that were energetically favorable: one of the sulfonyl oxygen atoms engaged in hydrogen bonds to Tyr 383 and Tyr 466. The second sulfonyl oxygen was positioned in hydrogen bonding distance to Tyr 383, and the sulfonamide nitrogen formed a hydrogen bond with the Asp 335 residue. Not surprisingly, this docking pose exhibited the highest Glide eModel score. In contrast, the energetically favored *cis* sulfonamide conformation could only be assumed by placing one of its sulfonyl oxygen atoms in close proximity to one of the oxygen atoms of the carboxylic acid side chain moiety of Asp 335 (2.9 Å), giving rise to an energetically unfavorable contact (Figure 4b). While showing a reduced eModel score, this binding pose exhibited the highest Glidescore. On the basis of these docking models, we hypothesize that the observed inactivity of **7** results from its inability to assume a low energy conformation *as well as* energetically favorable hydrogen bonding interactions with active site residues. This hypothesis is consistent with the strong conformational preference found for aromatic *cis* sulfonamides in protein−ligand complexes available in the Cambridge Crystallographic Database and the Protein Data Bank.[20] DFT/B3LYP calculations with a 6-31G** basis set revealed that there is a ~4 kcal energy difference favoring the *cis* sulfonamide conformation over the *trans* conformation after optimizing the geometries, holding the pyridyl/sulfonamide and sulfur−nitrogen bonds fixed. The energy difference between

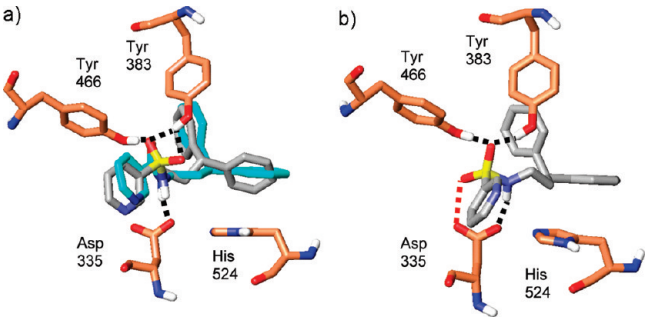

Figure 4. Putative binding modes of the inactive sulfonamide **7** (gray). (a) The high energy *trans* conformer displays energetically favorable hydrogen bonding interaction patterns with one sulfonyl oxygen engaged in hydrogen bonds (black dotted lines) to Tyr 383 and Tyr 466 and the second sulfonyl oxygen positioned in hydrogen bonding distance to Tyr 383. The sulfonamide nitrogen forms a hydrogen bond with Asp 335. The crystallographically obtained binding pose of **1** has been added for comparison (cyan). (b) The low energy *cis* sulfonamide conformation places one sulfonyl oxygen atom in close proximity to one of the oxygen atoms of the carboxylic acid side chain moiety of Asp 335, resulting in an energetically unfavorable contact (red dotted line).

cis and *trans* sulfonamides is consistent with earlier observations.[21] Allowing the pyridyl/sulfonamide to be optimized reduces the energy difference to ~2 kcal/mol; however, the energetically favored orientation of the pyridyl group would now lead to unfavorable interactions with Trp 336 (data not shown).

The importance of the left-hand side aromatic moiety of **1** was further delineated by evaluating analogues in which the 3-pyridyl ring was replaced with 2-pyridyl, 4-pyridyl, or phenyl (Table 3, entries **8**−**10**). The 4-pyridyl and phenyl derivatives **9** and **10** were both potent inhibitors of human and rat sEH, with IC_{50}s ranging from 5 to 8 nM. In contrast, the 2-pyridyl derivative displayed a loss in inhibitory potency averaging 12- to 14-fold relative to **1** (IC_{50} 100 and 43 nM for human and rat sEH, respectively). A plausible explanation for the reduced potency of **8** compared to **1** invokes an intramolecular hydrogen bond between the amide nitrogen and the 2-pyridyl nitrogen, leading the pyridyl ring system to adopt a coplanar conformation with the amide, thereby positioning its 2-pyridyl nitrogen in close proximity (3.3 Å) to the charged oxygen atoms of the Asp 335 side chain, resulting in a repulsive electrostatic interaction. This rationale was supported by comparing interaction energies between **1** and **8** within human sEH using a cocrystal structure of **1** (vide supra and Figure 5) and a model of **8** in the identical conformation as basis for the calculations. Using the OPLS2005 force field, a difference of 1.7 kcal/mol favoring **1** over **8** was calculated.

Evaluation of the in vitro metabolic stability profiles for these first sets of compounds (Tables 1 and 3) indicated rapid metabolism in human and rat liver microsomes (see Experimental Section for method). We anticipated that the observed rapid in vitro metabolism would translate to rapid clearance in vivo, hence limiting the sustained in vivo plasma exposure of these compounds. In accordance with this hypothesis, the plasma levels of **1** in the rat after oral administration were quickly depleted over time (data not shown), supporting the assumption that in vitro metabolic stability is predictive of in vivo clearance for this compound class. Careful examination of the in vitro metabolites generated from **1** in rat liver microsomes confirmed the extensive hydroxylation of the phenyl groups of the benzhydryl motif, which accounted for 76.9% of the total metabolite area. The bis-(4-fluorophenyl) analogue of **1** (Table 4, entry **11**) was synthesized to assess the impact of blocking the presumed metabolically vulnerable sites with fluoro atoms. However, examination of the in vitro metabolic profile of compound **11** revealed an apparent shift in the major route of metabolism to hydroxylation of the pyridine, now representing 76.1% of the total metabolite area. The stability of **11** in liver microsomes was assessed and found to be relatively short at 12 min in both human and rat liver microsomes (Table 4, entry **11**). Taken together, the shift to hydroxylation of the pyridine moiety and the fact that in vitro metabolism remained rapid for the fluorinated analogue suggested to us a propensity for metabolite switching.

The intrinsic potency of the bis-(4-fluorophenyl) analogue (Table 4, entry **11**) was evaluated and found to be unchanged relative to **1** (IC_{50}s 8 and 7 nM for human sEH and rat sEH, respectively). Hypothesizing that an increase in the overall polarity of these molecules might decrease first-pass metabolism, we decided to explore the effect of left-hand side substitution in the context of the bis-(4-fluorophenyl) modified right-hand side. Hence, the effect of small, polar substituents such as hydroxyl, trifluoroethoxy, cyano, and methanesulfonyl on benzhydryl moiety was examined in the context of the 3-pyridyl, 4-pyridyl, and phenyl left-hand sides. Potent inhibition of both human and rat sEH was observed for these derivatives with IC_{50}s ranging from 5 to 9 nM (Table 4, entries **12**−**16**). However, the examination of the in vitro half-lives of these compounds revealed large differences in metabolic stabilities as a result of left-hand side substitution. The inclusion of hydroxy and trifluoroethoxy substituents resulted in significant improvements in metabolic stabilities, most dramatically illustrated by the 6-(2,2,2-trifluoro-ethoxy)-nicotinamide analogue, **13**, which displayed a half-life in excess of 300 min in both human and rat liver microsomes. For compounds **14**, **15**, and **16**, the improvement in the metabolic stability in human microsomes was less dramatic and their half-lives in rat liver microsomes remained short at about 5 min. The identification of **13** as an in vitro metabolically stable and potent sEH inhibitor prompted us to assess its exposure in the rat. Following oral administration of **13** at 5 mg/kg, plasma concentrations were more sustained over time compared to **1** but remained low, reaching only 0.3, 0.2, 0.1, and 0 μM at the 1, 2, 4, and 6 h time points, respectively. Because of its poor aqueous solubility (less than 0.1 μg/mL at pH 7.4), **13** could not be evaluated for intestinal permeability in our in-house caco-2 assay.

The solid-state structure of the co-stucture of **1** and human sEH was determined to provide guidance for the design of compounds with increased metabolic stability and improved physicochemical properties while maintaining excellent binding characteristics. As shown previously, the active site in both rat and human sEH is formed by a channel in the protein between two large, solvent accessible pockets, with the active site tyrosine and aspartic residues encircling the ligand.[22−24] The costructure of **1** (Figure 5a) reveals the amide moiety of **1** positioned in a similar orientation to that observed previously for urea-based inhibitors, with the carbonyl oxygen directed toward the two tyrosines in the active site and the amide proton directed toward the aspartic acid. The structure shows the pyridine ring placed in the Trp 336 niche (adopting a similar nomenclature to that of Gomez et al.[24]) forming a π-stacking interaction with the tryptophan residue. The π-stacking interaction results in the pyridine ring adopting a similar orientation to that reported for the phenyl group in the

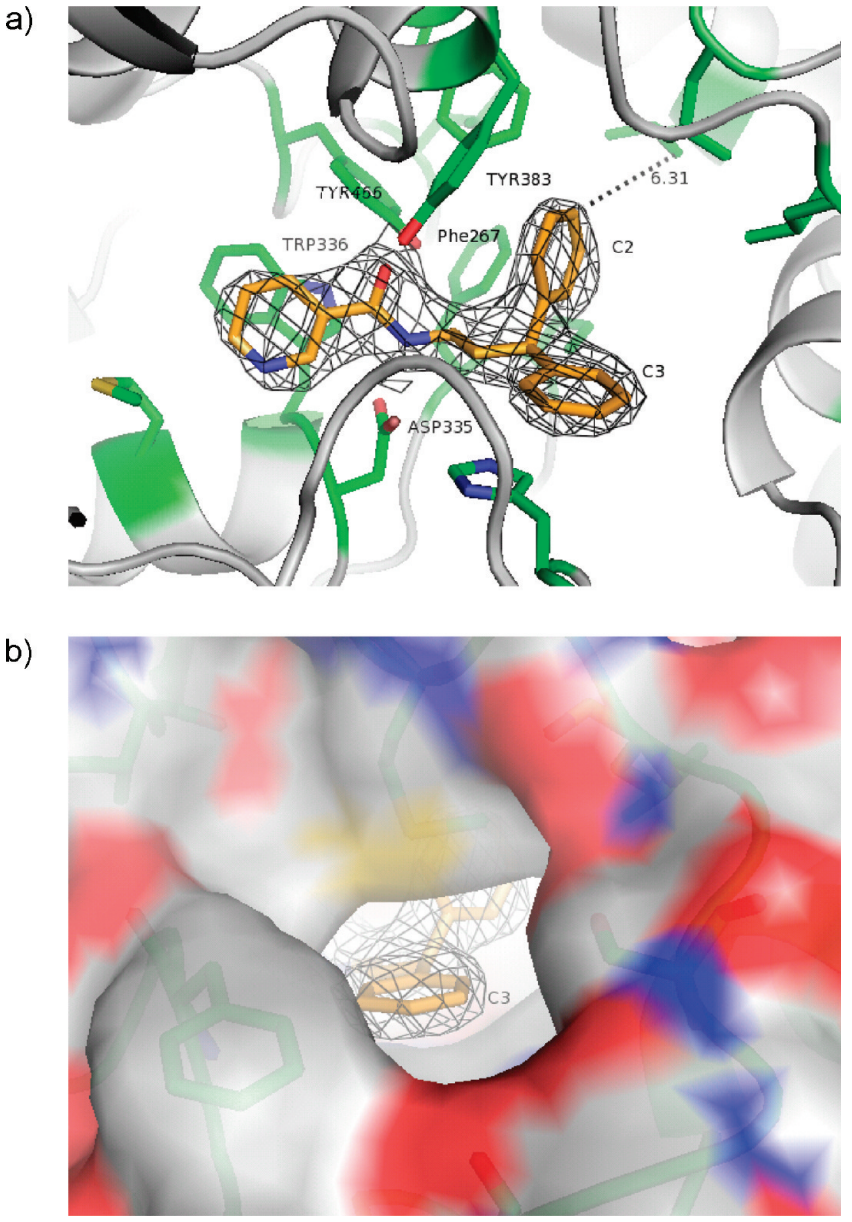

Figure 5. X-ray cocrystal structure of human sEH and **1**. (a) The $2f_o - f_c$ map contoured at 0.95σ showing the orientation of **1** in the binding site of human sEH. The catalytic residues Tyr 383, Tyr 466, and Asp 335 encircle the amide group of the ligand. Key residues involved in the catalytic mechanism are shown, as are some of the hydrophobic residues that line the Phe 267 pocket. The distance between the ligand and the rear of the Phe 267 pocket is indicated. (b) Surface representation illustrating how the environments of the C2 and C3 are very different. The C2 group is seen to be buried deep in the Phe 267 pocket, whereas the C3 phenyl is directed toward the solvent opening.

murine sEH *N*-cyclohexyl-*N*′-(4-iodophenyl) urea (CIU) structure.[25]

The trajectory of the propyl linker between the amide and benzhydryl motif is similar to that reported for the cyclohexyl urea compounds, with the molecule stretching from the active site triad toward the Phe 267 pocket. At this point, compound **1** bifurcates with one phenyl group, designated here as C2, directed toward the back of the Phe 267 pocket, and the other, referred here as C3, pointing toward the solvent opening. The phenyl directed to the rear of the pocket has a different trajectory from that seen in other sEH inhibitors: the cocrystal structure of human sEH with the CIU inhibitor does occupy some of the same space as the phenyl group, but the 4-iodo phenyl in that inhibitor is not directed as deeply toward the core of the protein. In the costructure with **1**, the C2 phenyl group is surrounded by hydrophobic residues (Phe 267, Pro 268, Phe 387, Leu 397, Leu 406, Leu 417, Leu 428, Leu 463). It is of interest to note that the C2 phenyl group does not fully occupy this pocket, which suggests that additional potency may be gained by more completely filling this pocket with hydrophobic substituents. The C3 phenyl group in **1** is directed toward the solvent opening of the Phe 267 pocket (Figure 5b). Previous inhibitor−sEH costructures have shown that this region of the protein can accommodate a variety of substituents, including cyclohexyl and carboxylic acid groups. In the costructure with **1**, the phenyl ring is positioned to allow π-stacking interaction with His 524. This interaction results in the ring lying close to one side of the pocket. In contrast, the cyclohexyl and acid moieties, seen in other structures, have tended to lie slightly more to the center of the pocket.

The fact that the two phenyl groups in the costructure of **1** occupy very different environments within the protein, one directed to a hydrophobic region of the protein, the other positioned in a more polar and solvent exposed environment,

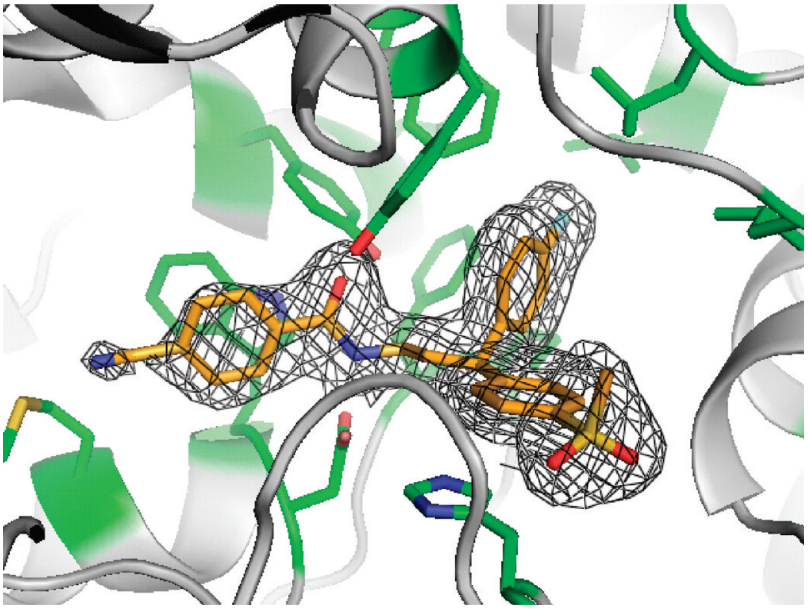

Figure 6. X-ray cocrystal structure of human sEH and **24**. The $2f_o - f_c$ map contoured at 0.95σ, showing that **24** binds in a similar mode to **1**. The structure reveals that the 4-fluorophenyl group is directed into the hydrophobic environment of the Phe 267 pocket, whereas the 4-methanesulphonyl substituted phenyl group is directed toward the solvent.

suggests that the introduction of asymmetry may be accommodated by the binding site. Asymmetric functionalization to exploit these differences might provide a path to the improvement of physicochemical properties as well as to improved potency. In pursuit of this idea, methanesulfonyl, a polar and nonionizable substituent, was introduced in the phenyl 4-position of the benzhydryl motif. The 4-fluoro substitution of the phenyl was maintained to prevent oxidative metabolism at this position. The effect of this combination of substituents on intrinsic potency and in vitro metabolic stability was probed by the synthesis of the racemic analogues **21**−**25** (Table 5) in which the left-hand side aryl pharmacophore was either unsubstituted or substituted with hydroxyl, 2,2,2-trifluoroethyloxy, cyano, or methanesulfonyl. The inclusion of the methanesulfonyl substituent on the benzhydryl motif of the nicotinamide derivative, **21**, resulted in an sEH inhibitor with largely uncompromised potency relative to **1** (IC_{50}s 8 and 14 nM for human and rat sEH, respectively). The 6-hydroxynicotinamide analogue of this compound (**22**) displayed a minor decrease in intrinsic potency against the human and rat sEH isoforms (IC_{50}s 16 and 29 nM, respectively), whereas the 2,2,2-trifluoroethoxy, cyano, and methanesulfonyl substituted analogues **23**, **24**, and **25** remained equipotent to **1**, with IC_{50}s ranging from 4 to 7 nM against human sEH and from 6 to 9 nM against the rat enzyme. These results indicate that the methanesulfonyl substitution is well accommodated by sEH.

As might be anticipated, the in vitro metabolism of the nicotinamide derivative, **21**, which lacks a left-hand side substituent, remained rapid in both human and rat liver microsomes, with half-lives of 6 and 12 min, respectively. In contrast, the in vitro half-lives for the analogues with polar left-hand side substituents (Table 5, **22**−**25**) ranged from a minimum value of 150 min to greater than 300 min, demonstrating that highly in vitro metabolically stable inhibitors *can* be achieved with this scaffold. The plasma levels of the sEH inhibitor **24** were determined in the rat after oral administration at 5 mg/kg (see Experimental Section for methods). Compound plasma exposure was 3.8, 3.5, 3.6, and 2.9 μM at the 1, 2, 4, and 6 h time-points, respectively, identifying this compound as a potent, in vitro metabolically stable sEH inhibitor, with sustained exposure in the rat.

To confirm that the unsymmetrically substituted analogue **24** bound in the expected orientation, a cocrystal structure with human sEH was obtained (Figure 6). The structure obtained confirmed the anticipated binding mode with very little difference in the position of the central amide core of the molecule in relation to the protein compared to the costructure with **1**. In the Trp 336 niche, the phenyl group of the 4-cyano-phenyl lies in a similar orientation to the 3-pyridyl of **1**. The cyano group is well accommodated within the large solvent-filled cavity of the Trp 336 niche, with Met 339 moving to accommodate the substituent. As expected, the 4-fluorophenyl group occupies the same space as the C2 phenyl in the costructure with **1**, the phenyl group lying in a very similar plane. It was noted earlier in the context of the costructure of **1** that the C2 phenyl group did not fully occupy the deep hydrophobic pocket. As anticipated, the 4-fluorophenyl group of **24** is accommodated by the pocket. The 4-methanesulfonyl substituted phenyl group, which was designed to capitalize on the more hydrophilic nature of the C3 pocket, lies in a similar orientation to the C3 group of **1**, with the methanesulfonyl substituent in close proximity to several polar groups including the side chains of Ser 425 and Asp 496 and the backbone carbonyl of Ser 412.

Our evaluation of the unsymmetrically substituted inhibitors **21**−**25** (Table 5) indicate that the polar methanesulfonyl substituent is well accommodated by sEH and that the observed improvements in microsomal stabilities lead to decreased in vivo clearance. To better understand the importance of asymmetry for the molecular recognition of sEH, a small set of enantiopure analogues was synthesized (Table 6, entries **S-24**, **R-24**, **S22**, and **R-22**). The corresponding enantiomers of **24** displayed a 2- to 4-fold difference in potency in favor of the *S*-enantiomer **S-24** (IC_{50} 8 and 6 nM, for human and rat isoforms, respectively) over the *R*-enantiomer **R-24** (IC_{50} 14 and 24 nM, for human and rat isoforms, respectively). These results are in agreement with our analysis of the solid-state structure, which predicts that the

Table 6. Inhibitory Potency (IC_{50}) against sEH and Stability in Microsomes ($t_{1/2}$) for Compounds **S-24**, **R-24**, **S-22**, and **R-22**[a]

	structure	human sEH IC_{50} [nM]	rat sEH IC_{50} [nM]	Hep G2 EC_{50} [nM]
S-24	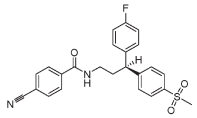	8	6	0.14
R-24	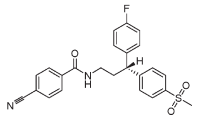	14	24	2.8
S-22	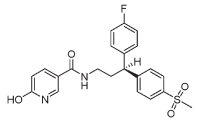	6	7	1.7
R-22	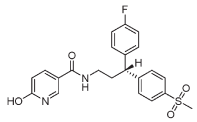	23	87	23

[a] Enantiopure compounds were synthesized to examine the importance of the asymmetry for the inhibition of sEH.

S-enantiomer will position the polar methanesulfonyl subtituent in the C3 pocket, leaving the 4-fluorophenyl group to occupy the relatively hydrophobic C2 pocket. The evaluation of the enantiomers of the intrinsically less potent **22**, **S-22**, and **R-22** confirmed the preference for placement of the hydrophilic methanesulfonyl substituent in the C3 binding pocket, in this case suggesting a greater, 4- to 12-fold, difference between the intrinsic potency of the *S*-enantiomer **S-22** (IC_{50}s 6 and 7 nM, for human and rat sEH) over the *R*-enantiomer **R-22** (IC_{50}s 23 and 87 nM, for human and rat sEH). Because of a limitation imposed by the affinity of the probe, the binding assay used in our studies can not provide an accurate ranking of compounds with IC_{50}s less than approximately 5 nM. To get a more accurate measure of the relative potencies of the advanced compounds **21**−**25** (Tables 5 and 6), their profiling was extended to include a cell-based assay in Hep G2 cells. Evaluation of the unsymmetrically substituted sEH inhibitors (Table 5, 21−**25**) in the cell-based assay confirmed the ranking observed in the fluorescence polarization assay (IC_{50}s 4, 6, 7 nM, respectively) and revealed that compounds **23**, **24**, and **25** are in fact of equal potency (EC_{50}s 0.3, 0.3, and 0.4 nM, respectively). In contrast, the evaluation of the enantiopure derivatives (Table 6, **S-24**, **R-24**, **S-22**, and **R-22**), revealed larger differences in the potency of the *S*- and *R*-enantiomers than estimated from the profiling in the fluorescence polarization assay. In fact, the data acquired in the cell-based assay suggests 14−20 fold differences in potency in favor of the *S*-enantiomers relative to the *R*-enantiomers with an EC_{50} of 0.14 nM for the *S*-enantiomer of **24** (**S-24**).

Conclusions

In conclusion, 4-cyano-*N*-[3-(4-fluorophenyl)-3-(4-methanesulfonyl-phenyl)-propyl]-benzamide, **24**, was identified as a potent sEH inhibitor with attractive in vitro stability profiles in rat and human liver microsomes and good oral exposure in the rat. The structure−activity relationship of the lead, **1**, reveals a relatively strict requirement to the distance between the central amide and benzhydryl motif, emphasizing the importance of the amide as a recognition element for sEH and suggesting a tight fit between the benzhydryl pharmacophore and the enzyme. In contrast, the structure−activity relationship reveals no particular structural requirements to the left-hand side aryl pharmacophore. Although not preferred, the transposition of this pharmacophore is allowed and substitution is well tolerated, as is the replacement of the 3-pyridyl pharmacophore with other (hetero)aryl groups. The above observations are corroborated by the costructure of **1** with sEH, in which the C3 phenyl appears to participate in a π-stacking interaction with His 524, and the C2 phenyl is in relatively close contact with several hydrophobic residues. The importance of the interaction between the central amide pharmacophore and the Tyr 466, Tyr 383, and Asp 335 residues can not be overemphasized and is illustrated by the diminished activity of the compound in which the amide configuration is reversed and the complete abrogation of activity for the sulfonamide derivative.

Optimization of the in vitro and in vivo metabolic parameters was accomplished using an integrated approach of metabolite identification and structure-based drug design aimed at preserving the inherently high inhibitory activity of this lead class. The identification of metabolically vulnerable sites and subsequent substitution with fluoro atoms led to the identification of an in vitro metabolically stable inhibitor, **13**. However, good in vitro metabolic stability for this compound is likely attained at the expense of suitable physicochemical properties and efficient in vivo absorption. Guided by the analysis of the costructure of **1** with human sEH, one fluorine atom was substituted for an additional polar substituent on the right-hand side benzhydryl motif, leading to the identification of a class of potent and in vitro metabolically stable sEH inhibitors. Compound **24** from this class was profiled extensively (Scheme 3) and was found to have a low potential for drug−drug interactions, good selectivity against EETs-generating CYP epoxygenases such as CYP2J2, CYP2C8, and CYP2C9, excellent in vitro microsomal stability, and high permeability in caco-2 cells (data not shown). The oral administration of **24** in the rat led to sustained compound exposure in plasma in the 3−4 μM range. Considering its overall profile, **24** is an appropriate candidate for in vivo pharmacological profiling.

Experimental Section

General Procedures. ^{1}H NMR spectra were recorded on a Bruker Avance (400 MHz) spectrometer. Chemical shifts are reported in ppm from tetramethylsilane with the solvent resonance as the internal standard ($CDCl_3$: 7.26 ppm). Data are reported as follows: chemical shifts, multiplicity (s = singlet, d = doublet, t = triplet, q = quartet, br = broad, m = multiplet), coupling constants (Hz), and integration. Liquid chromatography was performed using prepacked silica gel columns (Analogix Flash chromatograph RS-12 cartridges) of the indicated solvent system. Separation was achieved with a CombiFlash SQ16X chromatographer by Isco. All compounds described were of >95% purity. Purity was confirmed by analytical LC/MS recorded on a system consisting of a Waters ZQ mass spectrometer, an Agilent 1100 DAD, Sedex 85 ELS detector, and an Agilent 1100 HPLC system, equipped with a Zorbax SB-C18 rapid

Scheme 3. SAR Advancement, Illustrated by the Profiles of Compounds **1**, **13**, and **24**[a]

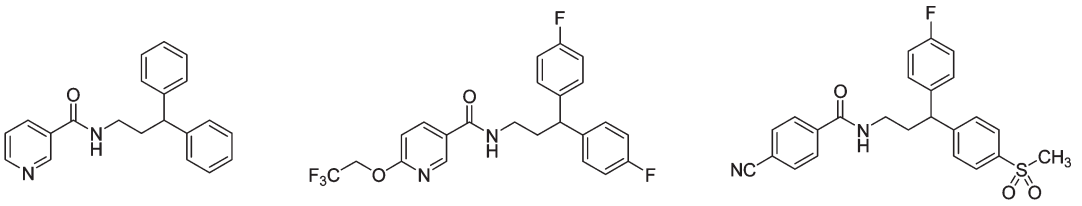

Compound 1

human sEH IC_{50} = 7 nM
rat sEH IC_{50} = 5 nM
Cell-based IC_{50} = 9 nM
2J2/2C9/2C19 IC_{50} = ND / 30 / 9 μM
HLM = 13 min
RLM = 3 min
Exposure, rat (5 mpk PO; 4h) = 0.0 μM

Compound 13

human sEH IC_{50} = 5 nM
rat sEH IC_{50} = 6 nM
Cell-based IC_{50} = < 1 nM
2J2/2C9/2C19 IC_{50} = 2 / 2 / 1 μM
HLM > 300 min
RLM > 300 min
Exposure, rat (5 mpk PO; 4h) = 0.1 μM

Compound 24

human sEH IC_{50} = 6 nM
rat sEH IC_{50} = 9 nM
Cell-based IC_{50} = < 0.14 nM
2J2/2C9/2C19 IC_{50} = 3 / 7 / 11 μM
HLM > 300 min
RLM = 150 min
Exposure, rat (5 mpk PO; 4h) = 3.6 μM

[a] The original screening hit 1 displayed high potency against both human and rat sEH and acceptable selectivity towards EETs forming CYPs but lacked in vitro metabolic stability. SAR to define an optimal scaffold for sEH inhibition, paired with substitution of the right-hand side benzhydryl motif with fluoro atoms, led to the identification of an in vitro metabolically stable inhibitor, **13**. However, good in vitro metabolic stability for this compound was attained at the expense of efficient in vivo absorption. Guided by the analysis of the co-structure of **1** with human sEH, one fluorine atom was substituted for an additional polar substituent, leading to the identification of compound **24**. This compound was found to have a low potential for drug−drug interactions, good selectivity against EETs-generating CYP epoxygenases such as CYP2J2, CYP2C8, and CYP2C9, excellent in vitro microsomal stability, and high and sustained compound exposure in the rat.

resolution cartridge (4.6 mm × 30 mm, 3.5 um). Elution started with 95% water (0.1% formic acid)/5% acetonitrile (0.1% formic acid) and ended with 95% acetonitrile (0.1% formic acid)/5% water (0.1% formic acid) and used a linear gradient at a flow rate of 2.5 mL/min. Final compounds were analyzed by high resolution mass spectrometry acquired on an Agilent LC/MSD TOF mass spectrometer equipped with an Agilent 1100 binary pump, WPALS auto sampler, Colcom oven, and DAD detector. Direct loop injection was performed using a 5 μL injection volume at a flow rate of 0.8 mL/min. Samples were dissolved in mobile phase, which consisted of 70/30 (A:B) (isocratic) with A 0.05% formic acid water (v/v) and B 0.05% formic acid in methanol (v/v). Detection was performed using positive ion ESI with a routine resolution of 6500 at *m*/*z* 322. Positive ion electrospray mass spectra of all final compounds were consistent with the proposed structures and molecular formula.

The following compounds were synthesized according to available literature procedures: 4,4-diphenyl-butylamine (Caldirola, 1992), 3,3-bis-(4-fluorophenyl)-propylamine (Buschauer, 1992), 4,4-diphenylbutyriuc acid (Miyano, 1990). The following chemicals were used as received: Hydroxybenzotriazole (Aldrich 36,244-1), 1-[3-(dimethylamino)propyl]-3-ethylcarbodiimde hydrochloride (Aldrich 16,146-2), diisopropylethylamine (Aldrich 38,764-9), nicotinic acid (Aldrich N785-0), 3,3-diphenyl-propylamine (Aldrich 13,629-8), 2,2-diphenyl-ethylamine (Aldrich D,20,670-9), phenethylamine (Aldrich 40,726-7), pyridine-2-carboxylic acid (picolinic acid) (Aldrich P4,280-0), 3-aminopyridine (Aldrich A-7,820-9), isonicotinic acid (Aldrich I-1,750-8), benzensulfonyl chloride (Aldrich 10,813-8), isonicotinic acid (Aldrich I-1,750-8), 2-(pyrdin-3-yl)-acetic acid hydrochloride (Aldrich P6,580-0), 6-hydroxynicotinic acid (Aldrich 12,875-9), 6-(2,2,2-trifluoro-ethoxy)-isonicotinic acid (Ryan Scientific RF 04860), 2-(2,2,2-trifluoro-ethoxy)-isonicotinic acid (Oakwood 017206), 4-cyanobenzoic acid (Aldrich C-8,980-3), 4-(methanesulfonyl)-benzoic acid (Aldrich 13,641-7), 4-fluorocinnamic acid (Aldrich 22,272-0), (*R*)-4-phenyl-2-oxazolidinone (Aldrich 40,245-1), (*S*)-4-phenyl-2-oxazolidinone (Aldrich 37,669-8), lithium diisopropyl amide (2 M in heptane/tetrahydrofuran/ethylbenzene) (Aldrich 36,179-8), copper(I)bromide-methylsulfide complex (Aldrich 23,050-2), methylsulfide (Aldrich 47,157-7), thioanisole magnesium bromide (0.5 M in tetrahydrofuran) (Aldrich 56,176-2).

General Procedure for Amide Bond Formation. To a solution of the carboxylic acid (1 equiv) in *N*,*N*′-dimethylformamide was added the amine (1.0 equiv), followed by the addition of 1-hydroxybenzotriazole (2.0 equiv), 1-[3-(dimethylamino)propyl]-3-ethylcarbodiimde hydrochloride (2.0 equiv), and diisopropylethylamine (3.0 equiv). The reaction was stirred overnight. The mixture was diluted with water and extracted twice with dichloromethane. The organic phase was evaporated in vacuo, and the crude product was purified by silica gel chromatography (0−5% methanol in dichloromethane) to provide desired product.

***N*-(3,3-Diphenyl-propyl)-nicotinamide (1).** This compound was synthesized on 0.47 mmol scale from nicotinic acid and 3,3-diphenyl-propylamine according to the general procedure for amide coupling to give the desired compound (110 mg, 73.3%). ^{1}H NMR δ: 8.75 (m, 1H), 8.71 (m, 1H) 8.06−8.01 (m, 1H), 7.40 (m, 1H), 7.29−7.35 (m, 8 H), 7.27−7.19 (m, 2H), 6.22 (brs, 1H), 4.06 (t, *J* = 7.7 Hz 1H) 3.55 (m, 2H), 2.47 (q, *J* = 7.1 Hz, 2H). HRMS: calcd for $C_{21}H_{20}N_2O + H^+$ 317.1654; found 317.1663.

***N*-(2,2-Diphenyl-ethyl)-nicotinamide (2).** This compound was synthesized on 1.63 mmol scale from nicotinic acid and 2,2-diphenyl-ethylamine according to the general procedure for amide coupling to give the desired compound (333 mg, 67.8%). ^{1}H NMR δ: 8.80 (m, 1H), 8.69 (m, 1H), 8.05 (m, 1H), 7.30−7.39 (m, 11 H), 6.25 (brs, 1H), 4.37 (t, *J* = 8.07 Hz, 1H), 4.15 (q, *J* = 8.10 Hz, 2H). HRMS: calcd for $C_{20}H_{18}N_2O + H^+$ 303.1497; found 303.1499.

***N*-(4,4-Diphenyl-butyl)-nicotinamide (3).** This compound was synthesized on 1.40 mmol scale from nicotinic acid and 4,4-diphenyl-butylamine according to the general procedure for amide coupling to give the desired compound (314 mg, 68.0%). ^{1}H NMR δ: 8.90 (m, 1H), 8.61 (m, 1H), 8.05 (m, 1H), 7.32 (m, 1H), 7.12−7.29 (m, 10H), 6.28 (brs, 1H), 3.86 (t, *J* = 7.8 Hz, 1H), 3.41 (q, *J* = 7.2 Hz, 2H), 2.06 (m, 2H), 1.54 (m, 2H). HRMS: calcd for $C_{22}H_{22}N_2O + H^+$ 331.1810; found 331.1802.

***N*-(3-Phenyl-propyl)-nicotinamide (4).** This compound was synthesized on 1.63 mmol scale from nicotinic acid and phenethylamine according to the general procedure for amide coupling to give the desired compound (257 mg, 65.8%). ^{1}H NMR δ: 8.88 (m, 1H), 8.72 (m, 1H), 8.06 (m, 1H), 7.30−7.39 (m, 6 H), 6.25 (brs, 1H), 3.52 (q, *J* = 6.89 Hz, 2H), 2.77 (t, *J* = 7.42 Hz, 2H), 2.02 (m, 2H). HRMS: calcd for $C_{15}H_{16}N_2O + H^+$ 241.1341; found 241.1339.

***N*-(3,3-Diphenyl-propyl)-2-pyridine-3-ylacetamide (5).** This compound was synthesized on 1.15 mmol scale from 2-(pyridin-3-yl)-acetic acid and 3,3-diphenyl-propylamine according to the general procedure for amide coupling to give the desired compound (309 mg, 81.2%). ^{1}H NMR δ: 8.55 (m, 2H), 7.71 (m, 1H), 7.29 (m, 6H), 7.20 (m, 5H), 5.25 (brs, 1H), 3.91 (t, J = 7.83 Hz, 1H), 3.40 (s, 2H), 3.24 (q, J = 6.36 Hz, 2H), 2.27 (m, 2H). HRMS: calcd for $C_{22}H_{22}N_2O$ + H^+ 331.1810; found 331.1809.

4,4-Diphenyl-*N*-(pyridin-3-yl)-butyramide (6). To 4,4-diphenylbutyric acid[16] (243 mg, 1.00 mmol) in dichloromethane (2 mL) was added oxalyl chloride (0.18 mL) and one drop of *N*,*N*′-dimethylformamide. The mixture was stirred at room temperature for 1 h, evaporated in vacuo, and redissolved in dichloromethane (2.50 mL). To this solution was added 3-aminopyridine (94 mg, 1.06 mmol) and triethylamine (0.25 mL, 1.80 mmol). The mixture was stirred at room temperature for 16 h, evaporated in vacuo, and purified on silica using dichlormethane/methanol (96:4) as the eluent. Fractions containing the product were pooled and evaporated in vacuo to give the desired product (186 mg, 55.3%). ^{1}H NMR δ: 8.53 (m, 1H), 8.27 (m, 2H), 7.44 (brs, 1H), 7.22−7.31 (m, 9H), 7.21 (m, 2H), 4.01 (t, J = 7.94 Hz, 1H), 2.53 (m, 2H), 2.39 (t, J = 7.69 Hz, 2H). HRMS: calcd for $C_{21}H_{20}N_2O$ + H^+ 317.1654; found 317.1632.

Pyridine-3-sulfonic Acid 3,3-(Diphenylpropyl)-amide (7). To a solution of benzenesulfonyl chloride (213 mg, 1.00 mmol) in dichloromethane (5 mL) was added 3,3-(diphenylpropyl)-amine (211 mg, 1.00 mmol) followed by triethylamine (0.28 mL, 2.00 mmol). The heterogeneous mixture was stirred at room temperature overnight, evaporated in vacuo, and purified on silica using silica using dichlormethane/methanol (95:5) as the eluent. Fractions containing the product were pooled and evaporated in vacuo to give the desired product (167 mg, 47.9%). ^{1}H NMR δ: 8.84 (m, 1H), 8.62 (m, 1H), 7.87 (m, 1H), 7.25 (m, 1H) 7.16−6.94 (m, 10H), 4.29 (t, 1H), 3.77 (t, 1H), 2.82 (q, 2H), 2.10 (q, 2H). HRMS: calcd for $C_{20}H_{20}N_2O_2S$ + H^+ 353.1324; found 353.1318.

Pyridine-2-carboxylic Acid (4,4-Diphenyl-propyl)-amide (8). This compound was synthesized on 0.47 mmol scale from pyridine-2-carboxylic acid and 4,4-diphenyl-propylamine according the general procedure for amide coupling to give the desired product (17 mg, 11.0%). ^{1}H NMR δ: 8.65 (m, 1H), 8.21 (m, 2H), 7.88 (m, 1H), 7.47 (m, 1H) 7.30−7.26 (m, 7 H), 7.2 (m, 2H), 4.08 (t, J = 7.87 Hz, 1H), 3.46 (q, J = 8.0 Hz, 2H), 2.45 (m, 2H). HRMS: calcd for $C_{21}H_{20}N_2O$ + H^+ 317.1654; found 317.1650.

***N*-(3,3-Diphenyl-propyl)-isonicotinamide (9).** This compound was synthesized on 0.47 mmol scale from isonicotinic acid and 3,3-diphenyl-propylamine according to the general procedure for amide coupling to give the desired product (93.9 mg, 62.7%). ^{1}H NMR δ: 8.69 (m, 2H), 7.44 (m, 2H), 7.30−7.39 (m, 8 H), 7.22 (m, 2H), 6.12 (brs, 1H), 4.06 (t, J = 7.72 Hz, 1H), 3.54 (q, J = 6.74 Hz, 2H), 2.46 (m, 2H). HRMS: calcd for $C_{21}H_{20}N_2O$ + H^+ 317.1654; found 317.1649.

***N*-[3,3-Bis-(4-fluorophenyl)-propyl]-benzamide (10).** This compound was synthesized on 0.82 mmol scale from benzoic acid and 3,3-diphenyl-propylamine according to the general procedure for amide coupling to give the desired product (231 mg, 89.5%). ^{1}H NMR δ: 7.50 (m, 2H), 7.33 (m, 3H), 7.20−7.31 (m, 8 H), 7.12 (m, 2H), 5.92 (brs, 1H), 3.96 (t, J = 7.70 Hz, 1H), 3.41 (q, J = 6.66 Hz, 2H), 2.35 (m, 2H). HRMS: calcd for $C_{22}H_{21}NO$ + H^+ 316.1701; found 316.1706.

***N*-[3,3-Bis-(4-fluorophenyl)-propyl]-nicotinamide (11).** This compound was synthesized on a 0.48 mmol scale from nicotinic acid and 3,3-bis-(4-fluorophenyl)-propylamine[17] according to the general procedure for amide coupling to give the desired compound (25 mg, 14.6%). ^{1}H NMR δ: 8.84 (brs, 1H), 8.61 (brs, 1H), 8.1−7.9 (d, 1H), 7.5−7.22 (m, 1H), 7.00−7.20 (m, 4H), 6.7−6.98 (m, 4H), 6.3−6.55 (m, 1H), 3.92 (t, 1H), 3.36 (q,2H), 2.29 (q, 2H).

***N*-[4,4-Bis-(4-fluorophenyl)-propyl]-6-hydroxy-nicotinamide (12).** This compound was synthesized on 2.02 mmol scale from 6-hydroxynicotinic acid and 3,3-bis-(4-fluorophenyl)-propylamine[17] according to the general procedure for amide coupling to give the desired product (480 mg, 64.4%). ^{1}H NMR δ: 8.17 (s, 1H), 7.80 (d, J = 8.8 Hz, 1H), 7.08 (q, J = 5.44 and 3.27 Hz, 4H), 6.96 (brs, 1H), 6.87 (t, J = 9.12 Hz, 4H), 6.55 (d, J = 9.12 Hz, 1H), 3.88 (t, J = 8.18 Hz, 1H), 3.31−3.22 (m, 2H), 2.23 (q, J = 6.95 and 7.77 Hz, 2H). HRMS: calcd for $C_{21}H_{18}F_2N_2O_2$ + H^+ 369.1415; found 369.1396.

***N*-[3,3-Bis-(4-fluorophenyl)-propyl]-6-(2,2,2-trifluoro-ethoxy)-nicotinamide (13).** This compound was synthesized on 0.20 mmol scale from 6-(2,2,2-trifluoro-ethoxy)-nicotinic acid and 3,3-bis-(4-fluorophenyl)-propylamine[17] according to the general procedure for amide coupling to give the desired product (31 mg, 34.0%). ^{1}H NMR δ: 8.34 (d, 1H), 7.86 (dd, J = 8.6 and 2.69 Hz, 1H), 7.16−7.09 (m, J = 5.58 Hz, 4H), 6.9−6.87 (m, J = 9.11 Hz, 4H), 6.8 (d, J = 8.75 Hz, 1H), 5.9−5.8 (m, 1H), 4.72 (q, J = 8.38 and 8.47 Hz, 2H), 3.92 (t, J = 8.1 Hz, 1H), 3.36 (q, J = 6.14 and 7.79 Hz, 2H), 2.28 (q, J = 6.87 and 7.60 Hz, 2H). HRMS: calcd for $C_{23}H_{19}F_5N_2O_2$ + H^+ 451.1445; found 451.1418.

***N*-[3,3-Bis-(4-fluorophenyl)-propyl]-2-(2,2,2-trifluoro-ethoxy)-isonicotinamide (14).** This compound was synthesized on 0.41 mmol scale from 2-(2,2,2-trifluoro-ethoxy)-isonicotinic acid and 3,3-bis-(4-fluorophenyl)-propylamine[17] according to the general procedure for amide coupling to give the desired product (61 mg, 34.0%). ^{1}H NMR δ: 8.14 (d, J = 5.37 Hz, 1H), 7.17−7.07 (m, 5H), 6.97−6.8 (m, 5H), 6.02−5.09 (m, 1H), 4.71 (q, J = 8.45 and 8.55 Hz, 2H), 3.91 (t, J = 8.27 Hz, 1H), 3.36 (q, J = 6.2 and 7.65 Hz, 2H), 2.27 (q, J = 6.77 and 7.67 Hz, 2H). HRMS: calcd for $C_{23}H_{19}F_5N_2O_2$ + H^+ 451.1445; found 451.1420.

4-Cyano-*N*-[3,3-bis-(4-fluorophenyl)-propyl]-benzamide (15). This compound was synthesized on 0.20 mmol scale from 4-cyanobenzoic acid and 3,3-bis-(4-fluorophenyl)-propylamine[17] according to the general procedure for amide coupling to give the desired product (75 mg, 98.0%). ^{1}H NMR δ: 7.64 (s, 4H), 7.17−7.09 (m, 4H), 6.96−6.86 (m, 4H), 6.01−5.09 (m, 1H), 3.92 (t, J = 7.9 Hz, 1H), 3.39 (q, J = 6.02 and 7.93 Hz, 2H), 2.29 (q, J = 6.76 and 7.85 Hz, 2H). HRMS: calcd for $C_{23}H_{18}F_2N_2O$ + H^+ 376.1387; found 376.1448.

***N*-[3,3-Bis-(4-fluorophenyl)-propyl]-4-methanesulfonyl-benzamide (16).** This compound was synthesized on 0.20 mmol scale from 4-methanesulfonyl benzoic acid and 3,3-bis-(4-fluorophenyl)-propylamine[17] according to the general procedure for amide coupling to give the desired product (73 mg, 84.1%). ^{1}H NMR δ: 7.89 (d, J = 8.32 Hz, 2H), 7.73 (d, J = 8.56 Hz, 2H), 7.17−7.09 (m, 4H), 6.97−6.86 (m, 4H), 6.13−6.00 (m, 1H), 3.93 (t, J = 7.9 Hz, 1H), 3.39 (q, J = 6.27 and 7.62 Hz, 2H), 2.99 (S, 3 H), 2.3 (q, J = 6.76 and 7.49 Hz, 2H). HRMS: calcd for $C_{23}H_{21}F_2NO_3S$ + H^+ 430.1288; found 430.1261.

3-(4-Fluorophenyl)-3-(4-methanesulfonyl-phenyl)-propylamine (20). To the *t*-Boc protected amine **19**[19] (1.20 g, 2.95 mmol) in methanol was added and HCl (aq, 6N) (8.0 mL) dropwise. The mixture was stirred at room temperature for 1 h and evaporated in vacuo to give a white solid that was triturated twice with diethyl ether and once with hexanes to give the desired compound as a colorless solid (872 mg, 86.1%). ^{1}H NMR (DMSO-d_6) δ: 7.85 (d, 2H), 7.80 (brs, 3H), 7.65 (d, 2H), 7.50 (m, 2H), 7.36 (m, 2H), 7.14 (m, 4H) 4.25 (m, 1H), 3.19 (s, 3H), 2.69 (m, 2H), 2.31 (m, 2H).

***N*-[3-(4-Fluorophenyl)-3-(4-methanesulfonyl-phenyl)-propyl]-nicotinamide (21).** This compound was synthesized on 0.55 mmol scale from nicotinic acid and 3-(4-fluorophenyl)-3-(4-methanesulfonyl-phenyl)-propylamine (**20**)[18] according to the general procedure for amide coupling to give the desired product (140 mg, 58.9%). ^{1}H NMR δ: 9.52 (brs, 1H), 8.64 (m, 1H), 8.50 (m, 1H), 7.88−7.47 (overlapping m, 3H), 7.66 (m, 1H), 7.45−7.41 (m, 2H), 7.24−7.14 (m, 2H), 7.00−6.91 (m, 2H), 4.18 (t, J = 7.30 Hz, 1H), 3.42−3.50 (m, 2H), 2.91 (s, 3H),

2.29−2.48 (m, 2H). HRMS: calcd for $C_{22}H_{21}FN_2O_3S$ 413.1335 + H^+; found 413.1316.

***N*-[3-(4-Fluorophenyl)-3-(4-methanesulfonyl-phenyl)-propyl]-6-hydroxy-nicotinamide (22).** To 6-hydroxynicotinic acid (139 mg, 1.00 mmol) was added thionyl chloride (1.8 mL) and the resulting mixture was heated at reflux for 2 h. The mixture was evaporated in vacuo, redissolved in dichloromethane (3 mL), and cooled to 0 °C. Triethylamine (0.24 mL) and 3-(4-fluorophenyl)-3-(4-methanesulfonyl-phenyl)-propylamine (**20**) (170 mg, 0.55 mmol) was added, and the mixture was allowed to come to room temperature and stirred for 2 h. The reaction was quenched by the addition of water (20 mL) and extracted twice with diethyl ether (2 × 10 mL). The combined organic phase was back-extracted with sodium bicarbonate (saturated, aq) (10 mL) and brine (10 mL), dried over magnesium sulfate, evaporated in vacuo, and purified on silica using dichlormethane/methanol (95:5) as the eluent. Fractions containing the product were pooled and evaporated in vacuo to give the desired product (107 mg, 25.0%). ^{1}H NMR δ: 12.01 (brs, 1H), 11.64 (brs, 1H), 8.06 (s, 1H), 7.76 (m, 1H), 7.71 (m, 2H), 7.37 (m, 2H), 7.13 (m, 2H), 6.93 (m, 1H), 6.83 (m, 1H), 6.35 (m, 1H), 4.04 (t, 1H), 3.29 (q, 2H), 2.98 (s, 3H), 2.32 (q, 2H). HRMS: $C_{22}H_{21}FN_2O_4S + H^+$ 429.1284; found 429.1259.

***N*-[3-(4-Fluorophenyl)-3-(4-methanesulfonyl-phenyl)-propyl]-6-(2,2,2-trifluoro-ethoxy)-nicotinamide (23).** This compound was synthesized on 0.553 mmol scale from 6-(2,2,2-trifluoro-ethoxy)-nicotinic acid and 3-(4-fluorophenyl)-3-(4-methanesulfonyl-phenyl)-propylamine (**20**) according to the general procedure for amide coupling to give the desired product (89 mg, 31.5%). ^{1}H NMR δ: 8.36 (d, J = 2.62 Hz, 1H), 7.90 (dd, J = 8.26 and 2.25 Hz, 1H), 7.79 (d, J = 8.39, 2H), 7.38 (d, J = 8.39, 2H), 7.18−7.10 (m, 2H), 7.00−6.89 (m, 2H), 6.83 (d, J = 8.77 Hz, 2H), 6.03−5.883.93 (m, 1H), 4.73 (q, J = 8.43 and 8.43 Hz, 2H), 4.03 (t, J = 7.30 Hz, 1 H), 3.37 (q, J = 6.20 and 7.81 Hz, 2H), 2.96 (s, 3H), 2.34 (q, J = 6.74 and 7.81 Hz, 2H). HRMS: calcd for $C_{24}H_{22}F_4N2O_4S$ 511.1315 + H^+; found 511.1320.

4-Cyano-*N*-[3-(4-fluorophenyl)-3-(4-methanesulfonyl-phenyl)-propyl]-benzamide (24). This compound was synthesized on 2.90 mmol scale from 4-cyano-benzoic acid and 3-(4-fluorophenyl)-3-(4-methanesulfonyl-phenyl)-propylamine (**20**) according to the general procedure for amide coupling to give the desired product (1.25 g, 98.5%). ^{1}H NMR δ: 7.43 (d, J = 8.37 Hz, 2H), 7.75 (q, J = 8.47 and 8.56 Hz, 4H), 7.27−7.21 (m, 2H), 7.04 (t, J = 8.66, 2H), 6.26−6.18 (m, 1H), d, J = 8.77 Hz, 2H), 4.13 (t, J = 7.85 Hz, 1H), 3.47 (q, J = 6.34 and 8.10 Hz, 2H), 3.047 (s, 3 H), 2.44 (q, J = 7.63 and 7.06 Hz, 2H). HRMS: calcd for $C_{24}H_{21}FN_2O_3S + H^+$ 437.1335; found 437.1309.

***N*-[3-(4-Fluorophenyl)-3-(4-methanesulfonyl-phenyl)-propyl]-4-methanesulfonyl-benzamide (25).** This compound was synthesized on 0.650 mmol scale from 4-methanesulfonyl-benzoic acid and 3-(4-fluorophenyl)-3-(4-methanesulfonyl-phenyl)-propylamine (**20**) according to the general procedure for amide coupling to give the desired product (279 mg, 87.0%). ^{1}H NMR δ: 7.88 (d, J = 8.36 Hz, 2H), 7.76 (t, J = 8.05 Hz, 4H), 7.38 (d, 8.33 Hz, 2H), 7.16 (m, 2H), 6.98- 6.90 (m, 2H), 6.28 (m, 1H), 4.05 (t, J = 7.97 Hz, 1H), 3.40 (q, J = 7.07 and 6.16 Hz, 2H), 3.00 (s, 3 H), 2.94 (s, 3H), 2.45- 2.28 (m, 2H). HRMS: calcd for $C_{24}H_{24}FNO5S + H^+$ 490.1158; found 490.1126.

3-[3-(4-Fluorophenyl-)acryloyl]-(*R*)-4-phenyl-oxazolidin-2-one (27a). To a precooled (−10 °C) solution of 4-fluorocinnamic acid (**26**) (2.96 g, 17.8 mmol) in tetrahydrofuran (80 mL) was added trietheylamine (2.98 mmol, 21.4 mmol) followed by the slow addition of pivaloyl chloride (2.36 g, 19.6 mmol). The mixture was stirred at −10 °C for 30 min, cooled to −78 °C, and a solution of the anion of (*R*)-4-phenyl-2-oxazolidinone (generated from (*R*)-4-phenyl-2-oxazolidinone (3.20 g, 19.6 mmol) in tetrahydrofuran (90 mL) at −78 °C by treatment with lithium diisopropyl amide (2 M in heptane/tetrahydrofuran/ethylbenzene) (8.47 mL, 16.9 mmol) for 30 min) was added while at −78 °C. The resulting mixture was stirred at −78 °C for 1 h, allowed to come to room temperature, and poured into 0.5N aq hydrochloric acid (80 mL). The aqueous solution was extracted with ethyl acetate (2 × 50 mL) and the combined organic fractions washed with sodium bicarbonate (aq, saturated) (75 mL), water (50 mL), brine (50 mL), dried over sodium sulfate, and evaporated in vacuo. The crude product was purified on silica using heptane/ethyl acetate (3:1) as the eluent. Fractions containing the product were pooled and evaporated in vacuo to give desired compound (4.10 g, 77.7%). ^{1}H NMR δ: 7.85 (d,1H), 7.72 (d, 1H) 7.60 (m, 2H), 7.39 (m, 5H), 7.09 (m, 2H) 5.58 (dd, 1 H), 4.76 (m, 3H), 4.35 (dd, 1H).

(*S*)-3-[3-(4-Fluorophenyl)-3-(4-methylsulfanyl-phenyl)-propionyl]-(*R*)-4-phenyl-oxazolidin-2-one (28a). To a precooled (−40 °C) solution of copper(I)bromide methylsulfide complex (4.06 g, 19.8 mmol) in tetrahydrofuran (40 mL) was added dimethylsulfide (20 mL), followed by the slow addition of thioanisole magnesium bromide (0.5 M in tetrahydrofuran) (79.0 mL, 39.5 mmol). The mixture was allowed to warm to −20 °C over 15 min and a solution of **27a** (4.10 g, 13.2 mmol) in tetrahydrofuran (20 mL) was added dropwise over 1 h. The resulting solution was stirred at −20 °C for 1 h, allowed to come to room temperature, stirred overnight, and poured into saturated aq ammonium chloride (200 mL). The mixture was extracted with ethyl acetate (2 × 150 mL) and the combined organic fractions washed with ammonium hydroxide (2 × 15% aq) (150 mL), water (150 mL), brine (150 mL), dried over sodium sulfate, and evaporated in vacuo. The crude product was purified on silica using heptane/ethyl acetate (3:1) as the eluent. Fractions containing the product were pooled and evaporated in vacuo to give desired compound (5.17 g, 90.0%) as a colorless solid. ^{1}H NMR δ: 6.9−7.3 (m,,13H), 5.33 (dd, 1 H), 4.61 (m, 1H), 4.55 (m, 1H), 4.21 (dd, 1H), 3.78 (dd, 1H), 3.64 (dd, 1H), 2.43 (s, 3H).

(*S*)-3-(4-Fluorophenyl)-3-(4-methylsulfanyl-phenyl)-propan-1-ol (29a). To a precooled solution of **28a** (5.10 g, 11.7 mmol) in tetrahydrofuran (60 mL) was added water (10 mL) followed by the portionwise addition of sodium borohydride (1.17 g, 30.2 mmol), keeping the temperature under 10 °C. The resulting solution was allowed to come to room temperature, stirred overnight, tetrahydrofuran was evaporated in vacuo, and water (50 mL) was added. The solution was extracted with ethyl acetate (2 × 50 mL) and the combined organic fractions washed with brine (50 mL), dried over sodium sulfate, and evaporated in vacuo. The crude product was purified on silica using heptane/ethyl acetate (1:1) as the eluent. Fractions containing the product were pooled and evaporated in vacuo to give desired compound (2.45 g, 76.0%) as a colorless oil. ^{1}H NMR δ: 7.0−7.3 (m,6H), 6.88 (m, 2H), 4.05 (m, 1H), 3.45 (m, 2H), 2.90 (brs, 1H), 2.35 (s, 3H), 2.18 (m, 2H).

(*S*)-3-(4-Fluorophenyl)-3-(4-methylsulfanyl-phenyl)-propyl-azide (30a). To a precooled (−10 °C) solution of **29a** (2.45 g, 8.86 mmol) in dichloromethane (40 mL) was added triethylamine (1.48 mL, 10.6 mmol) followed by the slow addition of toluenesulfonyl chloride (2.03 g, 10.6 mmol). The mixture was stirred at −10 °C for 1 h, stirred overnight at room temperature, and evaporated in vacuo. The residue was dissolved in *N*,*N*-dimethylformamide (20 mL), sodium azide (1.15 mg, 16.6 mmol) was added, the mixture was stirred at room temperature overnight, and water (40 mL) was added. The aqueous phase was extracted with ethyl acetate (2 × 20 mL) and the combined organic fractions washed with water (20 mL), brine (20 mL), dried over sodium sulfate, and evaporated in vacuo. The crude product was purified on silica using heptane/ethyl acetate (3:1) as the eluent. Fractions containing the product were pooled and evaporated in vacuo to give desired compound (2.52 g, 89.6%) as a colorless oil. ^{1}H NMR δ: 7.1−7.21 (m,6H), 6.95 (m, 2H), 4.05 (t, 1H), 3.22 (t, 2H), 2.45 (s, 3H), 2.35 (q, 2H).

(*R*)-3-(4-Fluorophenyl)-3-(4-methylsulfoxide-phenyl)-propyla-zide (31a). To **30a** (2.52 g, 8.36 mmol) was added a mixture of glacial acetic acid (10 mL) and hydrogen peroxide (30% aq)

(8 mL). The resulting solution was stirred at room temperature for 1 h and water (20 mL) added, the aq phase was extracted twice with ethyl acetate (2 × 20 mL), and the organic phase was washed with brine (15 mL), dried over sodium sulfate, and evaporated in vacuo to give the desired product (1.27 g 45.0%). ^{1}H NMR δ: 7.62 (d, 1H), 7.39 (d, 1H), 7.20 (m, 1H), 7.00 (m, 1H), 4.13 (m, 1H), 3.25 (t, 2H), 2.70 (s, 3H), 2.30 (q, 2H).

Boc-(*S*)-3-(4-fluorophenyl)-3-(4-methanesulfoxide-phenyl)-propylamine (32a). To **31a** (1.27 g, 3.76 mmol) was added methanol (15 mL) and Pd (10% on carbon) (200 mg), and the mixture was stirred under hydrogen overnight, filtered through celite (washing with methanol), and evaporated in vacuo to desired compound as a colorless oil, which was used without further purification (1.15 g, 47.3%). To the crude amine (1.15 g, 4.00 mmol) in dichloromethane (15 mL) was added di-*tert*-butyl dicarbonate (Boc-anhydride) (490 mg, 5.20 mmol) and triethylamine (1.0 mL, 7.20 mmol). The mixture was stirred at room temperature for 4 h, and the organic phase was washed with aq HCl (1N) (10 mL) and evaporated to give a colorless oil (1.54 g, 100%). ^{1}H NMR δ: 7.58 (d, 2H), 7.40 (d, 2H), 7.20 (m, 2H), 7.00 (m, 2H), 4.55 (m, 1H), 4.01 (m, 1H) 3.15 (m, 2H), 2.71 (s, 3H), 2.2 (m, 2H) 1.40−1.60 (m, 9 H).

Boc-(*S*)-3-(4-fluorophenyl)-3-(4-methanesulfonyl-phenyl)-propylamine (33a). To a solution of **32a** (1.54 g, 4.00 mmol) in 80 mL of chloroform is added aluminum oxide (4.19 g, 41.0 mmol) pretreated with 0.84 mL of water. The resulting suspension was stirred and treated with 8.37 g of oxone (13.6 mmol) and refluxed for 23 h. The reaction was cooled to room temperature, filtered, and evaporated in vacuo to give an amorphous solid. The crude product was purified on silica using heptane/ethyl acetate as the eluent (1.62 g, 100%). ^{1}H NMR δ: 7.82 (d, 2H), 7.40 (d, 2H), 7.18 (m, 2H), 7.00 (m, 2H), 4.71 (m, 1H), 4.05 (m, 1H) 3.07 (m, 2H), 3.02 (s, 3H), 2.05 (m, 2H) 1.42 (s, 9 H); 91% ee chiral HPLC Chiracel Chiralpak AD-H, 4.6 mm × 250 mm, 85% heptane, 15% ethanol, 1.0 mL/min 25 °C. Retention time 34.5 minor, 37.1 major.

(*S*)-3-(4-Fluorophenyl)-3-(4-methanesulfonyl-phenyl)-propylamine (S-20). To a solution of **33a** (1.62 g, 4.00 mmol) in 6 mL of dichloromethane was added 12 mL of trifluororacetic acid followed by 0.60 mL of water. The resulting mixture was stirred for 2 h and 15 min and the solvents evaporated in vacuo. The resulting oil was taken up in dichloroethane and evaporated in vacuo. The oil was then taken up in 15 mL of dichloroethane and *para*-toulenesulfonic acid was added (760 mg, 4.00 mmol) in one portion. The reaction was the evaporated in vacuo and the resulting residue triturated with ether and heptane. The solid was filtered and dried in vacuo to give a the desired compound (0.94 g, 49.0%) as a colorless solid. ^{1}H NMR (DMSO-d_6) δ: 7.85 (d, 2H), 7.80 (brs, 3H), 7.65 (d, 2H), 7.50 (m, 2H), 7.36 (m, 2H), 7.14 (m, 4H) 4.25 (m, 1H), 3.19(s, 3H), 2.69 (m, 2H), 2.31 (m, 2H).

3-[3-(4-Fluorophenyl-)acryloyl]-(*S*)-4-phenyl-oxazolidin-2-one (27b). To a precooled (−10 °C) solution of 4-fluorocinnamic acid (**26**) (4.77 g, 28.7 mmol) in tetrahydrofuran (40 mL) was added trietheylamine (4.80 mmol, 34.4 mmol) followed by the slow addition of pivaloyl chloride (3.89 g, 31.6 mmol). The mixture was stirred at −10 °C for 30 min, cooled to −78 °C, and a solution of the anion of (*S*)-4-phenyl-2-oxazolidinone (generated from (*S*)-4-phenyl-2-oxazolidinone (5.15 g, 31.56 mmol) in tetrahydrofuran (60 mL) at −78 °C by treatment with lithium diisopropyl amide (2 M in heptane/tetrahydrofuran/ethylbenzene) (15 mL, 30.00 mmol) for 30 min) was added while at −78 °C. The resulting mixture was stirred at −78 °C for 1 h, allowed to come to room temperature, and poured into 0.5N aq hydrochloric acid (75 mL). The aqueous solution was extracted with ethyl acetate (2 × 50 mL) and the combined organic fractions washed with sodium bicarbonate (aq, saturated) (75 mL), water (50 mL), brine (50 mL), dried over sodium sulfate, and evaporated in vacuo. The crude product was purified on silica using heptane/ethyl acetate (3:1) as the eluent. Fractions containing the product were pooled and evaporated in vacuo to give desired compound (3.96 g, 43.4%). Spectroscopic data identical to those of **27a**.

(*R*)-3-[3-(4-Fluorophenyl)-3-(4-methylsulfanyl-phenyl)-propionyl]-(*S*)-4-phenyl-oxazolidin-2-one (28b). To a precooled (−40 °C) solution of copper(I)bromide methylsulfide complex (3.92 g, 19.08 mmol) in tetrahydrofuran (40 mL) was added dimethylsulfide (20 mL), followed by the slow addition of thioanisole magnesium bromide (0.5 M in tetrahydrofuran) (76.3 mL, 38.16 mmol). The mixture was allowed to warm to −20 °C over 15 min, and a solution of **27b** (3.96 g, 12.72 mmol) in tetrahydrofuran (20 mL) was added drowise over 1 h. the resulting solution was stirred at −20 °C for 1 h, allowed to come to room temperature, stirred overnight, and poured into saturated aq ammonium chloride (200 mL). The mixture was extracted with ethyl acetate (2 × 150 mL), and the combined organic fractions washed with ammonium hydroxide (2 × 15% aq) (150 mL), water (150 mL), brine (150 mL), dried over sodium sulfate, and evaporated in vacuo. The crude product was purified on silica using heptane/ethyl acetate (3:1) as the eluent. Fractions containing the product were pooled and evaporated in vacuo to give desired compound (4.80 g, 87.0%) as a colorless solid. ^{1}H NMR δ: 6.9−7.3 (m,,13H), 5.35 (dd, 1 H), 4.61 (m, 1H), 4.55 (m, 1H), 4.20 (dd, 1H), 3.80 (dd, 1H), 3,65 (dd, 1H), 2.25 (s, 3H).

(*R*)-3-(4-Fluorophenyl)-3-(4-methylsulfanyl-phenyl)-propan-1-ol (29b). To a precooled solution of **28b** (4.75 g, 10.91 mmol) in tetrahydrofuran (60 mL) was added water (10 mL) followed by the portionwise addition of sodium borohydride (0.89 g, 23.45 mmol), keeping the temperature under 10 °C. The resulting solution was allowed to come to room temperature, stirred overnight, tetrahydrofuran was evaporated in vacuo, and water (40 mL) was added. The solution was extracted with ethyl acetate (2 × 50 mL) and the combined organic fractions washed with water (50 mL), brine (50 mL), dried over sodium sulfate, and evaporated in vacuo. The crude product was purified on silica using heptane/ethyl acetate (1:1) as the eluent. Fractions containing the product were pooled and evaporated in vacuo to give desired compound (2.11 g, 70.0%) as a colorless oil. Spectroscopic data identical to those of **28a**.

(*R*)-3-(4-Fluorophenyl)-3-(4-methylsulfanyl-phenyl)-propyl-azide (30b). To a precooled (−10 °C) solution of **29b** (2.10 g, 7.60 mmol) in dichloromethane (30 mL) was added triethylamine (1.27 mL, 9.12 mmol) followed by the slow addtion of toluenesulfonyl chloride (1.74 g, 9.12 mmol). The mixture was stirred at −10 °C for 1 h, stirred overnight at room temperature, and evaporated in vacuo. The residue was dissolved in *N*, *N*-dimethylformamide (15 mL), sodium azide (0.99 g, 15.19 mmol) was added, the mixture was stirred at room temperature overnight, and water (40 mL) was added. The aqueous phase was extracted with ethyl acetate (2 × 20 mL) and the combined organic fractions washed with water (20 mL), brine (20 mL), dried over sodium sulfate, and evaporated in vacuo. The crude product was purified on silica using heptane/ethyl acetate (3:1) as the eluent. Fractions containing the product were pooled and evaporated in vacuo to give desired compound (2.25 g, 93.3%) as a colorless oil. Spectroscopic data identical to those of **29a**.

(*R*)-3-(4-Fluorophenyl)-3-(4-methylsulfoxide-phenyl)-propyl-azide (31b). To **30b** (2.25 g, 7.09 mmol) was added a mixture of glacial acetic acid (10 mL) and hydrogen peroxide (30% aq) (8 mL). The resulting solution was stirred at room temperature for 1 h and water (20 mL) added, the aqueous phase was extracted twice with ethyl acetate (2 × 20 mL), the organic phase washed with brine (15 mL), dried over sodium sulfate, and evaporated in vacuo to give the desired product (1.27 g, 57.0%). Spectroscopic data identical to those of **31a**.

(*R*)-3-(4-Fluorophenyl)-3-(4-methanesulfoxide-phenyl)-propylamine (32b). To **31b** (1.00 g) was added methanol (15 mL) and Pd (10% on carbon) (167 mg), the mixture was stirred under hydrogen overnight, filtered through celite (washing with methanol), and evaporated in vacuo to desired compound as a

colorless oil (0.50 g, 24.0%). To this amine (0.500 g, 1.72 mmol) in dichloromethane (10 mL) was added di-*tert*-butyl dicarbonate (Boc-anhydride) (490 mg, 2.23 mmol) and triethylamine (0.430 mL, 3.00 mmol). The mixture was stirred at room temperature for 4 h and the organic phase washed with aq HCl (1N) (10 mL) and evaporated to give the desired compound (672 mg, 100%) as a colorless oil. Spectroscopic data identical to those of **32a**.

Boc-(*R*)-3-(4-Fluorophenyl)-3-(4-methanesulfonyl-phenyl)-propylamine (33b). To a solution of the above sulfoxide (**32b**) (885 mg, 2.26 mmol) in 35 mL of chloroform was added 1.8 (17.6 mmol) g of aluminum oxide pretreated with 360 μL of water. The resulting suspension was treated with 3.6 g of oxone (5.8 mmol) and refluxed for 24 h. The reaction was cooled to room temperature, filtered, and the solvents evaporated in vacuo. The crude product was purified on silica using heptane/ethyl acetate as the eluent 0.94 g (2.26 mmol, 100%). Spectroscopic data same as **33a**; 82% ee chiral HPLC Chiracel Chiralpak AD-H, 4.6 mm × 250 mm, 85% heptane, 15% ethanol, 1.0 mL/min 25 °C. Retention time 34.4 major, 37.2 minor).

(*R*)-3-(4-Fluorophenyl)-3-(4-methanesulfonyl-phenyl)-propylamine (R-20). To a solution of **33b** 0.94 g (2.30 mmol) in 5 mL of dichloromethane was added 10 mL of trifluororacetic acid followed by 0.500 mL of water. The resulting mixture was stirred for 1 h and solvents removed in vacuo. The oil was taken up in 15 mL of dichloroethane and *para*-toluenesulfonic acid (396 mg, 0.94 mmol) was added in one portion. The reaction was the evaporated in vacuo, and the resulting residue triturated with ether and heptane. The solid was filtered and dried in vacuo to give the desired compound (1.01 g, 91.0%) as colorless solid. ^{1}H NMR (DMSO-d_6) δ: 7.85 (d, 2H), 7.80 (brs, 3H), 7.65 (d, 2H), 7.50 (m, 2H), 7.36 (m, 2H), 7.14 (m, 4H) 4.25 (m, 1H), 3.19(s, 3H), 2.69 (m, 2H), 2.31 (m, 5H).

(*S*)-4-Cyano-*N*-[3-(4-fluorophenyl)-3-(4-methanesulfonyl-phenyl)-propyl]-benzamide (S-24). This compound was synthesized on 0.21 mmol scale from 4-cyano-benzoic acid and (*S*)-3-(4-fluorophenyl)-3-(4-methanesulfonyl-phenyl)-propylamine (**S-20**) according to the general procedure for amide coupling to give the desired compound (50 mg, 54.9%). ^{1}H NMR δ: 7.69−7.77 (m, 6H), 7.38 (m, 2H), 7.15 (m, 2H), 7.69 (m, 2H), 6.36 (brt, 1H), 4.04 (t, J = 7.42 Hz, 1H), 3.36 (q J = 6.14 Hz, 2H), 3.94 (s, 3H), 2.34 (m, 2H). HRMS: calcd for $C_{24}H_{21}FN_2O_3S$ 437.1335; found 437.1325.

(*R*)-4-Cyano-*N*-[3-(4-fluorophenyl)-3-(4-methanesulfonyl-phenyl)-propyl]-benzamide (R-24). This compound was synthesized on 0.21 mmol scale from 4-cyano-benzoic acid and (*R*)-3-(4-fluorophenyl)-3-(4-methanesulfonyl-phenyl)-propylamine (**R-20**) (according to the general procedure for amide coupling to give the desired compound (51 mg, 55.0%). ^{1}H NMR δ: 7.69−7.77 (m, 6H), 7.38 (m, 2H), 7.15 (m, 2H), 7.69 (m, 2H), 6.36 (brt, 1H), 4.04 (t, J = 7.42 Hz, 1H), 3.36 (q J = 6.14 Hz, 2H), 3.94 (s, 3H), 2.34 (m, 2H). HRMS: calcd for $C_{24}H_{21}FN_2O_3S$ 437.1335; found 437.1318.

(*S*)-*N*-[3-(4-Fluorophenyl)-3-(4-methanesulfonyl-phenyl)-propyl]-6-hydroxy-nicotinamide (S-22). This compound was synthesized on 0.42 mmol scale from 6-hydroxynicotinic acid and (*S*)-3-(4-fluorophenyl)-3-(4-methanesulfonyl-phenyl)-propylamine (**S-20**) according to the general procedure for amide coupling to give the desired compound (100 mg, 56.0%). ^{1}H NMR δ: 8.20 (brs, 1H), 7.80 (m, 1H), 7.79 (m, 2H), 7.42 (m, 3H), 7.19 (m, 2H), 6.96 (m, 2H), 6.45 (m, 1H), 4.10 (brt, J = 8.5 Hz, 1H), 3.33 (m, 2H), 3.10 (s, 3H), 2.37 (m, 2H). HRMS: calcd for $C_{22}H_{21}FN_2O_4S + H^+$ 429.1284; found 429.1259.

(*R*)-*N*-[3-(4-Fluorophenyl)-3-(4-methanesulfonyl-phenyl)-propyl]-6-hydroxy-nicotinamide (R-22). This compound was synthesized on 0.42 mmol scale from 6-hydroxynicotinic acid and (*R*)-3-(4-fluorophenyl)-3-(4-methanesulfonyl-phenyl)-propylamine (**R-20**) according to the general procedure for amide coupling to give the desired compound (95 mg, 53.2%). ^{1}H NMR δ: 8.20 (brs, 1H), 7.80 (m, 1H), 7.79 (m, 2H), 7.42 (m, 3H), 7.19 (m, 2H), 6.96 (m, 2H), 6.45 (m, 1H), 4.10 (brt, J = 8.5 Hz, 1H), 3.33 (m, 2H), 3.10 (s, 3H), 2.37 (m, 2H). HRMS: calcd for $C_{22}H_{21}FN_2O_4S + H^+$ 429.1284; found 429.1282.

In Vitro Molecular Assay for Inhibition of Human or Rat sEH. This assay identifies compounds that inhibit the binding interaction of either human or rat soluble epoxide hydrolase with a tetramethyl rhodamine-labeled probe. Test compounds were dissolved and serially diluted in DMSO, with final dilution in assay buffer (20 mM TES, 200 mM NaCl, 0.05% w/v CHAPS, 1 mM TCEP, pH = 7.0) to achieve 1% DMSO in the assay. Test compounds were dispensed into a black, flat-bottom 96-well plate. Positive controls were reaction mixtures containing no test compound; negative controls (blanks) were reaction mixtures containing a reference inhibitor. The reaction was started with the addition of a mixture of either human or rat sEH (final assay concentration is 10 nM) and probe (final assay concentration is 2.5 nM). The reaction was mixed by briefly shaking the plate on an orbital shaker, and the plates were incubated in the dark for 30 min at room temperature. Fluorescence polarization is measured on an LJL Analyst using a 530 nm excitation filter, a 580 nm emission filter, and a 561 nm dichroic mirror. Concentration−response data were fitted to a 4-parameter equation to determine IC_{50} values.

In Vitro Cellular Assay for Inhibition of sEH in Human Hep G2 Cells. This assay identifies compounds that inhibit the ability of soluble epoxide hydrolase to convert 14,15-epoxy-eicosatienoic acid to 14,15-dihydroxyeicosatrienoic acid in human HepG2 cells. HepG2 cells, grown in low glucose DMEM supplemented with 10% fetal bovine serum, were seeded at 20000 cells/well in 96-well poly D-lysine-coated plates 18 h prior to the assay. On the day of the assay, test compounds were dissolved and serially diluted in DMSO, with final dilution in assay medium (low glucose DMEM containing 6.6 μg/mL BSA) to achieve a 0.3% DMSO in the assay. Positive controls were wells containing no test compound; negative controls (blanks) were reaction mixtures containing a reference inhibitor. The growth medium was aspirated from the cells, they were washed once with phosphate buffered saline containing calcium and magnesium, and assay medium was added. Test compounds were dispensed into the plates, which were then placed in a humidified incubator at 37 °C with 5% CO_2 for 30 min. After addition of 14,15-epoxy-eicosatienoic acid to a final concentration of 330 nM, the plates were placed in a humidified incubator at 37 °C with 5% CO_2 for 2 h. Quantitation of 14,15-dihydroxyeicosatrienoic acid in the supernatants was performed using a commercially available ELISA kit (cat. no. DH 21 from Detroit R&D, Inc.). Concentration−response data were fitted to a 4-parameter equation to determine IC_{50} values.

Assessment of Stability in Rat and Human Liver Microsomes. The stability of the compounds in rat and human liver microsomes were determined by calculating the half-lives of compounds from two time points (0 and 30 min). The incubation consisted of a microsomal content was 1 mg/mL, a NADPH (nicotinamide adenine dinucleotide phosphate-oxidase) concentration of 2.5 mM, and a compound concentration of 1 μM. All compounds were preincubated at 37 °C for 5 min on a Tecan Genesis. Following preincubation, NADPH was added and samples were incubated at 37 °C for 30 min on a Tecan Genesis. Reactions were stopped when 80 uL of each sample was collected at 0 and 30 min and crashed with 160 μL of cold acetonitrile. The crashed samples were filtered and analyzed by LC/MS/MS. The half-life of disappearance of parent molecule ($t_{1/2}$) was calculated by dividing 0.693 by the slope of parent loss.

Methods for Computational Analyses of Compounds 7 and 8. Glide 4.0 docking[26] in standard precision mode was used to predict putative binding modes of **7** and **8** in the catalytic site of human sEH represented by an in-house crystal structure. The protein was prepared for docking using 500 steps of Polak−Ribier conjugant gradient minimization in the presence of compound **1** constraining heavy atoms with a force constant of

100 kcal/mol/Å^2. Two hydrogen bonding constraints to Asp 335 and to either Tyr 383 or Tyr 466 were required for accepted docking solutions. Standard conditions were chosen for all other docking parameters. Force field calculations were performed using the OPLS2005 force field as implemented by Schrodinger Inc. Geometry optimization calculations were performed using DFT/B3LYP with a 6-31G** basis set using Jaguar6.5.[27]

Method for Identification of in Vitro Metabolites. Additional incubations were optimized to identify the phase I metabolites of 1 and 15. The incubations consisted of a microsomal content of 1 mg/mL, a NADPH concentration of 2.5 mM, and a compound concentration of 10 μM. The mixtures were preincubated at 37 °C for 4 min. The reactions were initiated by the addition of NADPH. Control samples were prepared in the absence of NADPH, where additional buffer was added to equal the volume of NADPH added to the test compound mixtures. The reactions were continued for 30 min and stopped by the addition of 1 mL of ice cold acetonitrile. The resulting mixtures were vortexed for 10 s and centrifuged to remove particulates. The control and test compound supernatants (1 mL each) were dried under nitrogen at 40 °C. The dried supernatants were reconstituted in H_2O/acetonitrile/acetic acid (70/30/0.1, v/v/v), vortexed, and centrifuged. A LC/MS/MS system consisting of a Hewlett-Packard Series 1100 system (auto injector, pump, and diode array detector) and a Micromass Ultima triple quadrupole mass spectrometer was used for the metabolite ID experiments. LC/MS/MS experiments were conducted to obtain full scan spectra and product ion spectra for the protonated parent ions of the compounds and the phase I metabolites.

Assessment of Compound Exposure in Rats. Male Sprague−Dawley rats (Charles River, Co.) were purchased precannulated (jugular catheter) in order to facilitate precise blood sampling times to increase throughput and to reduce the stress on the animals caused by serial bleedings. Three fed rats were dosed orally with one compound at a dose of 5 mg/kg. Blood was collected into heparin-containing tubes serially from each animal at 1, 2, 4, and 6 h postdosing and centrifuged to generate plasma. The plasma samples were stored at −20 °C until analysis. The plasma concentrations were obtained by extraction of the compound from an aliquot of rat plasma by precipitation of proteins with acetonitrile and quantitation by LC/MS/MS. The LC/MS/MS system consisted of a Hewlett-Packard Series 1100 pump, Leap Technologies injector, and an Applied Biosystems API4000 mass spectrometer. The LC/MS/MS system was operated in multireaction monitoring (MRM) mode.

Expression and Purification of Human sEH. Human soluble epoxide hydrolase was obtained using a baculovirus expression system. The cells were lysed using sonication in a buffer containing 20 mM MOPS (3-(*N*-morpholino)propanesulfonic acid) pH 7.4, 75 mM NaCl, 10% glycerol 1 mM EGTA (ethylene glycol tetraacetic acid), 1 mM EDTA (ethylenediaminetetraacetic acid), 3 mM DTT (dithiothreitol), 1 mM PMSF (phenylmethylsulfonyl fluoride), μg/mL pepstatin, and 4 μg/mL leupeptin. The lysate was clarified by centrifugation and loaded onto a benzyl-thio sepharose column that had been equilibrated with 20 mM MOPS pH 7.4, 75 mM NaCl, 10% glycerol, 1 mM EDTA, 3 mM DTT. The protein was eluted using the same buffer as used for equilibration plus 1 mM *trans*-1,3-diphenyl-2,3-epoxypropan-1-one (chalcone oxide). The eluted protein was then concentrated and dialyzed against a buffer containing 100 mM sodium phosphate pH 7.4, 50 mM NaCl and 3 mM DTT. Plasma levels of **1** and **13** were determined using a 1% CMC/0.2% Tween80/98.8% water formulation, whereas a 80% PEG 400/20% pH2 30 mM citric acid formulation was used for the determination of plasma levels of **24**.

Crystallization and Structure Determination. Crystals of apo sEH were obtained using the hanging drop method. Drops were prepared by combining 5 μL of the protein at a concentration of 12 mg/mL with 5 μL of a well solution containing: 0.2 M lithium sulfate, 36% PEG 3350, and 0.1 M Tris pH 8.4 and 0.5 μL of 0.006 mM β-D-hexadecyl maltoside. Crystals were observed to grow within 1 week at 4 °C. A 100 mM stock solution of compounds **1** and **24** were prepared in DMSO. Prior to addition of compound, crystals were transferred to a stabilizing solution containing 0.2 M lithium sulfate, 40% PEG 3350, and 0.1 M Tris pH 8.4. The stock compound solution was added to the drop containing the protein to give a final concentration of 10 mM. The crystals were then allowed to soak for 1 week at 4 °C. Cryoprotection of the crystals was achieved by gradually adding sucrose to the stabilizing solution to a final concentration of 20%. The crystals were then flash frozen in liquid nitrogen.

Diffraction data for the cocrystal containing **1** was collected on the SGX-CAT beamline at the Advanced Photon Source using a wavelength of 0.929 Å and a MAR165 CCD 165. Diffraction data for the cocrystal containing **24** was collected on the PXI beamline Swiss Light Source using a MAR 225 CCD. Data reduction was performed using Mosflm. Molecular replacement was performed using the program AMORE in conjunction with the apo human soluble epoxide structure 1S8O.pdb. Refinement and model building was performed using CNX and Phenix. Initial refinement of the model was performed with no waters present in the model. Following the addition of water molecules to the model and subsequent rounds of refinement, the ligand was added to the model. Table 7 contains the data reduction and refinement statistics of the final models.

Table 7. Refinement Statistics

compd	**1**	**24**
resolution range, Å	38.1−2.5	36.25−1.95
unit cell, Å P6(5)22	$a = b = 92.609$	$a = b = 92.410$
($\alpha = \beta = 90$; $\gamma = 120$)	$c = 244.046$	243.983
reflections measured/unique	1321310/23208	3243810/183207
completeness (outer shell)	99(100)	98(96)
reflections work/test	21903/1115	42950/2271
I/σ (outer shell)	4.7(0.9)	11.7(1.6)
no. of atoms	4378	4500
no. of waters	37	152
R/R_{free}	22.6/29.1	21.4/25.5
rmsd (Å) bonds	0.004	0.008
rmsd (deg) angles	0.8	1.1

Acknowledgment. We thank Michael August and Lori Patnaude for performing the high-throughput screen of our compound collection against sEH.

References

(1) Larsen, B. T.; Campbell, W. B.; Guttermann, D. B. Beyond Vasodilation: Nonvasomotor Roles of Epoxyeicosatrienoic Acids in the Cardiovascular System. *Trends Pharmacol. Sci.* **2007**, *28* (1), 32–38.
(2) Spector, A. A.; Norris, A. N. Action of Epoxyeicosatrienoic Acids on Cellular Function. *Am. J. Cell Physiol.* **2007**, *292*, 996–1012.
(3) Schmelzer, K. R.; Inceoglu, B.; Kubala, L.; Kim, I.-H.; Jinks, S. L.; Eiserich, J. P.; Hammock, B. D. Enhancement of Antinociception by Coadministartion of Nonsteroidal Anti-inflammatory Drugs and Soluble Epoxide Hydrolase Inhibitors. *Proc. Natl. Acad. Sci. U.S.A.* **2006**, *103* (37), 13646–13651.
(4) Yu, Z.; Xu, F.; Huse, L. M.; Morriseau, C.; Draper, A. J.; Newman, J. W.; Parker, C.; Graham, L.; Engler, M. M.; Hammock, B. D.; Zeldin, D. C.; Kroetz, D. L. Soluble Epoxide Hydrolase regulates Hydrolysis of Vasoactive Epoxyeicosatrienoic Acids. *Circ. Res.* **2000**, *87*, 992–998.
(5) Fang, X.; Weintraub, N. L.; McCaw, R. B.; Hu, S.; Harmon, S. D.; Rice, J. B.; Hammock, B. D.; Spector, A. A. Effect of soluble epoxide hydrolase inhibition on epoxyeicosatrienoic acid metabolism in human blood vessels. *Am. J. Physiol.* **2004**, *287*, 2412–2420.
(6) Spector, A. A.; Fang, X.; Snyder, G. D.; Weintraub, N. L. Epoxyeicosatrienoic acids (EETs): metabolism and biochemical function. *Prog. Lipid Res.* **2004**, *43*, 55–90.

(7) Dorrance, A. M.; Rupp, N.; Pollock, D. M.; Newman, J. W.; Hammock, B. D.; Imig, J. D. An epoxide hydrolase inhibitor 12-(3-Adamantan-1-yl-ureido)dodecanoic acid (AUDA) reduces ischemic cerebral infarct size in stroke-prone spontaneously hypertensive rats. *J. Cardiovasc. Pharm.* **2005**, *46*, 842–848.
(8) Olearczyk, J. J.; Field, M. B.; Kim, I.-H.; Morisseau, C.; Hammock, B. D.; Imig, J. D. Substituted adamantyl-urea inhibitors of the soluble epoxide hydrolase dilate mesenteric resistance vessels. *J. Pharm. Exp. Ther.* **2006**, *318*, 1307–1314.
(9) Zhao, X.; Yamamoto, T.; Newman, J. W.; Kim, I.-H.; Watanabe, T.; Hammock, B. D.; Stewart, J.; Pollock, J. S.; Pollock, D. M.; Imig, J. D. Soluble Epoxide Hydrolase Inhibition Protects the Kidney from Hypertension-Induced Damage. *J. Am. Soc. Nephrol.* **2004**, *15*, 1244–1253.
(10) Morisseau, C.; Goodrow, M. H.; Dowdy, D.; Zheng, J.; Greene, J. F.; Sanborn, J. R.; Hammock, B. D. Potent urea and carbamate inhibitors of soluble epoxide hydrolases. *Proc. Natl. Acad. Sci. U.S.A.* **1999**, *96*, 8849–8854.
(11) Kim, I.-H.; Morisseau, C.; Watanabe, T.; Hammock, B. D. Design, Synthesis and Biological Activity of 1,3-Disubstituted Ureas as Potent Inhibitors of Soluble Epoxide Hydrolase of increased water solubility. Optimization of Amide-Based Inhibitors of Soluble Epoxide Hydrolase with Improved Water Solubility. *J. Med. Chem.* **2004**, *47*, 2110–2122.
(12) Kim, I.-H.; Heirtzler, F. R.; Morisseau, C.; Nishi, K.; Tsai, H.-J.; Hammock, B. D. Optimization of Amide-Based Inhibitors of Soluble Epoxide Hydrolase with Improved Water Solubility. *J. Med. Chem.* **2005**, *48*, 3621–3629.
(13) Kim, I.-H.; Tsai, H.-J.; Nishi, K.; Kasagami, T.; Morisseau, C.; Hammock, B. D. 1,3-Disubstituted Ureas Functionalized with Ether Groups are Potent Inhibitors of the Soluble Epoxide Hydrolase with Improved Pharmacokinetic Properties. *J. Med. Chem.* **2007**, *50*, 5217–5226.
(14) Hwang, S. H.; Tsai, H.-J.; Liu, J.-Y.; Morisseau, C.; Hammock, B. D. Orally Bioavailable Potent Soluble Epoxide Hydrolase Inhibitors. *J. Med. Chem.* **2007**, *50*, 3825–3840.
(15) Caldirola, P. M.; van der Goot, H.; Timmerman, H. New prenylamine analogs: synthesis and calcium(2+)-entry blocking activity *Eur. J. Med. Chem.* **1992**, *27*, 571–579.
(16) Miyano, S.; Tatsuoka, T.; Suzuki, K.; Imao, K.; Satoh, F.; Ishihara, T.; Hirotsu, I.; Kihara, T.; Hatta, M.; et al. The synthesis and antilipidperoxidation activity of 4,4-diarylbutylamines and 4,4-diarylbutanamides. *Chem. Pharm. Bull.* **1990**, *38*, 1570–1574.
(17) Buschauer, A.; Friese-Kimmel, A.; Baumann, G.; Schunack, W. Synthesis and histamine H2 agonistic activity of arpromidine analogs: replacement of the pheniramine-like moiety by nonheterocyclic groups. *Eur. J. Med. Chem.* **1992**, *27*, 321–230.
(18) Taylor, S. J.; Netherton, M. R. Synthesis of the Benzhydryl Motif via a Suzuki−Miyaura Coupling of Arylboronic Acids and 3-Chloroacrylonitriles. *J. Org. Chem.* **2006**, *71*, 397–400.
(19) Muegge, I.; Rarey, M. Small Molecule Docking and Scoring. In *Reviews in Computational Chemistry*; Boyd, D. B., Lipkowitz, K. B., Eds.; Wiley-VCH: New York, 2001; Vol 17, pp 1−60,
(20) Berman, H. M.; Westbrook, J.; Feng, Z.; Gilliland, G.; Baht, T. N.; Weissig, H.; Shindyalov, I. N.; Bourne, P. E. The Protein Data Bank. *Nucleic Acid Res.* **2000**, *28*, 235–242.
(21) Hao, M.-H.; Haq, O.; Muegge, I. Torsion Angle Preferences and Energetic of Small-Molecule Ligands Bound to Proteins. *J. Chem. Inf. Model.* **2007**, *47*, 2242–2252.
(22) Gomez, G. A.; Morisseau, C.; Hammock, B. D.; Christianson, D. W. Structure of Human Epoxide Hydrolase Revels Mehanistic Inferences on Bifuctional Catalysis in Epoxide and phosphate Ester Hydrolysis. *Biochemistry* **2004**, *43*, 4716–4723.
(23) Argiriadi, M. A.; Morisseau, C.; Hammock, B. D.; Christianson, D. W. Detoxification of environmental mutagens and carcinogens: structure, mechanism and evolution of liver epoxide hydrolase. *Proc. Natl. Acad. Sci. U.S.A.* **1999**, *96*, 10637–10642.
(24) Gomez, G. A.; Morisseau, C.; Hammock, B. D.; Christianson, D. W. Human soluble epoxide hydrolase: structural basis of inhibition by 4-(3-cyclohexylureido)-carboxylic acids. *Protein Sci.* **2006**, *15*, 58–64.
(25) Argiriadi, M. A.; Morisseau, C.; Goodrow, M. H.; Dowdy, D. L.; Hammock, B. D.; Christianson, D. W. Binding of Alkyurea Inhibitors to Epoxide Hydrolase Implicates Active Site Tyrosines in Substrate Activation. *J. Biol. Chem.* **2000**, *275*, 15265–15270.
(26) Friesner, R. A.; et al. Glide: a new approach for rapid, accurate docking and scoring. 1. Method and assessment of docking accuracy. *J. Med. Chem.* **2004**, *47*, 1739–1749.
(27) *Jaguar, version 6.5*; Schrodinger LLC: New York, 2006.